5 Generation of bubbles and foams

> You don't start to play your guitar thinking you're going to be running an organization that will maybe generate millions.
>
> Keith Richards, www.quoteauthors.com/keith-richards-quotes/

5.1 Introduction

There are a number of methods for generating foams, and these have been reasonably well documented throughout the literature. They may be classified into two groups; the first involves the entrapment of air bubbles from the atmosphere and this can be achieved by relatively simple techniques such as shaking, pouring, circulation, sparging (introduction of gas using frits), etc. The second method involves artificially producing gas bubbles by physical methods (e.g. by nucleation or electrolysis) or chemical methods, which are commonly exploited in the production of polymer foams and involve the use of so-called blowing agents. These are chemical compounds that decompose or react to produce gas bubbles. While it is difficult to control the bubble size using physical methods of bubble formation, with chemical methods it is much easier to achieve a narrow-size distribution along with a high generation rate. Many different types of gases are used for foam generation, but it is important to recognize that foams generated with less soluble gases, such as N_2 or air, will coarsen more slowly than foams produced with more soluble gases such as CO_2 since gas diffusion through the soap films is largely determined by the gas solubility and the diffusion coefficient. In traditional foaming processes such as froth flotation, mechanical air entrapment methods are frequently used since they are relatively inexpensive, whereas in the production of material foams more sophisticated chemical processes have been developed.

5.2 The adsorption of surfactant on the freshly generated bubbles

The initial step in the generation of bubbles and foams involves the formation of a gas/ liquid interface. This process involves work which can be quantified as the product of the

interfacial tension and the increase in area of the interface; it be expressed by the equation

$$W = \gamma \Delta A \tag{5.1}$$

where ΔA is the created interfacial area and γ is the surface tension of the freshly produced bubbles. In water, bubbles have a high interfacial energy and become instantly unstable. Therefore, it is essential that surfactant adsorbs at the interface and reduces the surface tension and stabilizes the bubble. The adsorption kinetics plays an important role in the stabilization of the bubble, and the surfactant molecules need to rapidly diffuse from the bulk solution to the bubble interface. From a theoretical viewpoint, the progressive adsorption process at a new surface in the absence of stirring or an energy barrier can be followed by using Fick's diffusion theory, as described, according to Ward (1), by the equation

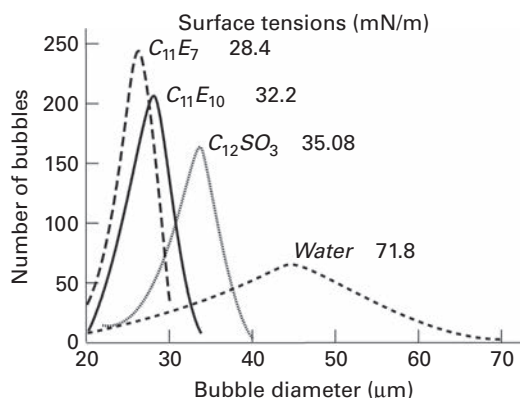$$\Gamma = 2C_{\mathrm{S}}(Dt/\pi)^{1/2} \tag{5.2}$$

where Γ is the number of molecules/cm^2 adsorbed on the surface of the bubble, D is the diffusion coefficient (cm^2/s) of the surfactant, C_{s} is the concentration of surfactant in the bulk concentration in mol/l, and t is the diffusion time in seconds.

An average value of the quantity of surfactant needed in the bulk solution to produce stable foams in the absence of stirring can be estimated. For small molecules, if we assume a value for the diffusion coefficient to be about 10^{-6} cm^2/s, the amount of surfactant needed to give an equilibrium surface concentration to be about 2×10^{14} molecules/cm^2 and the times involved in foam production to be in the range of 0.001 to 0.1 s (taking a mean value of 0.01 s), then the concentration of surfactant required in the bulk solution to give a stable foam would be approximately 1.7×10^{-3} M.

However, the above calculation only applies for the stabilization of a bubble by small surfactant molecules diffusing to the air/water interface, because for larger molecules other factors that can delay the process are involved. For example, high molecular weight polymeric surfactants and proteins are adsorbed more slowly than short-chain low molecular weight surfactants since they have higher diffusion coefficients. Adsorption energy barriers need to be considered, particularly with strongly charged molecules, where electrostatic repulsive barriers also reduce the diffusion rates. The foam production method is an important factor because stirring and turbulent flow can also reduce the adsorption rate on the expanding bubbles. Therefore, it is important to ensure fairly high concentrations of surfactant are present in the solution for the successful generation of bubbles and foams under rapid stirring and shaking.

5.3   Bubble size and distribution

It follows from the Laplace–Young equation (Chapter 1) that the nature of the surfactant and the surface tension of the solution play an important role in defining the bubble size
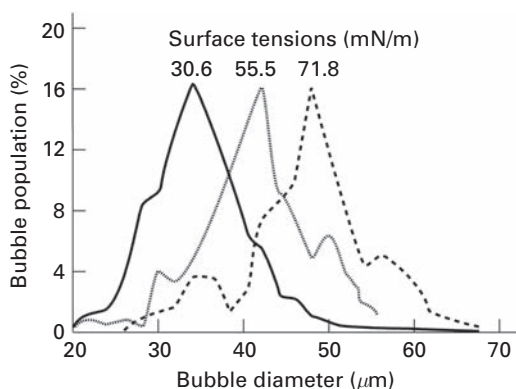
Fig. 5.1   Bubble size distribution versus population of different surfactant solutions at concentrations near the CMC compared to water. From ref (2).
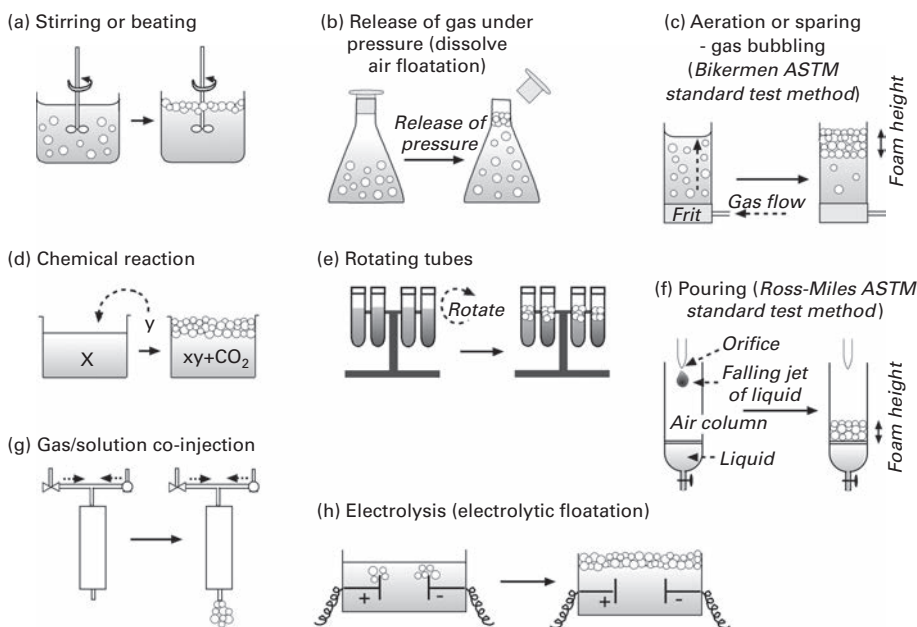
and size distribution during bubble generation. This was demonstrated in experiments carried out by Rao and Stenius (2) for a series of surfactants in which the molecular size, the hydrophobic/hydrophilic balance of the surfactant and the surface tension of the solution were changed during the generation step. Bubbles were initially generated by passing gas through a porous plate which was the base of a glass cell containing surfactant solution. The size distribution and population of bubbles were determined by image analysis using a laser technique with a CCD camera, which enabled images of the bubbles produced in the cell to be captured, digitized and processed. Using this method, a minimum population of 600 bubbles could be sized, counted and characterized about 10 ms after release.

In Fig. 5.1, the bubble size distribution in surfactant solutions (at concentrations near the CMC of each surfactant) is shown and compared to that in pure water. These concentration values were chosen to ensure maximum packing of each surfactant at the bubble interface. From these results it can be seen that as the surface tension of the solution is reduced, the average maximum bubble size becomes smaller as anticipated but also the bubble size distribution becomes narrower. In addition, it was noted that the lower the equilibrium surface tension, the more hydrophobic the surfactant. In the case of pure water, the bubble size distribution was considerably wider and the average maximum bubble size larger.

In Fig. 5.2, results are shown for different concentrations of $C_{11}E_{10}$ surfactant. In this case, it can be seen that as the solution concentration increases and the surface tension is reduced, the average bubble size decreases but the size distribution becomes more or less constant. These results suggest that while the average maximum bubble size is dependent on the concentration of the surfactant, the size distribution is more dependent on the molecular packing and structure of the surfactant adsorbed at the bubble interface. In addition, from this study, a linear relationship – in accordance with the theoretical predictions of the Laplace–Young equation – was established between the average maximum bubble size and the equilibrium surface tension of the solution.

Fig. 5.2   Bubble size distribution in $C_{11}E_{10}$ surfactant solution at two different concentrations compared to water. From ref (2).
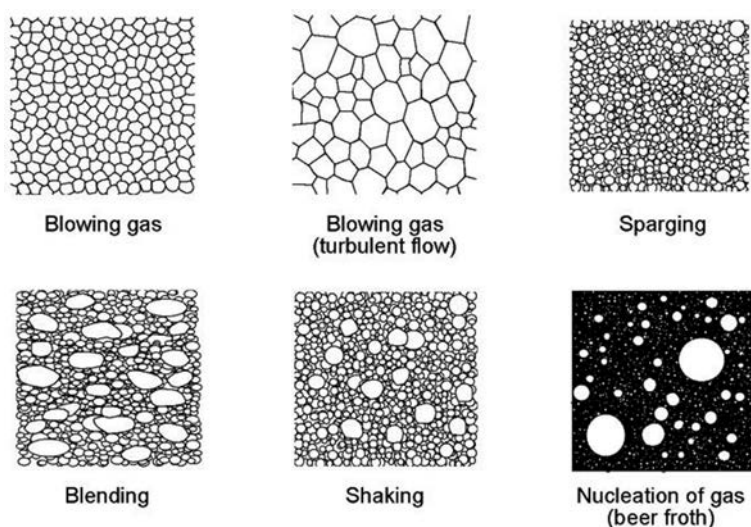

Fig. 5.3   An overview of commonly used methods for the generation of bubbles and foams.

5.4   Overview of foam generation techniques

The generation of foams is essentially a non-equilibrium process, with commonly used methods based on shaking, sparging or stirring. In Fig. 5.3, a brief outline is shown of some of the methods of generating foams which are then described in detail in the subsequent sections.

The type of foam produced greatly depends on the generation process, with parameters such as the velocity of the process, gas intake (over-run), turbulence,

Fig. 5.4 Samples of 2D foams (obtained from squeezing between glass plates). The foams were generated by various processes and show the influence of the generation technique on bubble size and cell structure. From ref (3).

temperature, viscosity of the liquid, type of surfactant and the rate of diffusion of surfactant to the interface having some influence on the bubble size, stability and foam microstructure. Weaire and Hutzler (3) compared the distribution of bubble sizes of foams prepared by several different generation processes. Samples were collected and squeezed between glass slides, enabling the bubble size distribution of two-dimensional foams to be recorded. The results are illustrated in Fig. 5.4, and a general indication of the range of bubble shapes and sizes obtained by the different processes is provided.

5.5 Mechanical methods

The simplest traditional mechanical methods of foam generation usually involve agitating the gas/liquid interface by beating with a paddle, rotary stirrer or flipping. In the kitchen, beating devices and foam blenders are frequently used for many different food recipes which often include egg whites, whipped cream, ice cream and mousse. However, it is almost impossible to control the gas intake using these methods, and usually large bubbles are formed with wide size distributions (ranging from 0.1 to 3 mm). During the initial agitation, entrainment of gas takes place from the surface and large bubbles are produced, but these are broken down by continuous shearing forces until equilibrium is established. The difficulties in producing small bubbles can be explained by the fact that deformation of a large bubble to produce smaller bubbles is opposed by an increase in Laplace pressure. To carry out an effective disruption process, a high external stress (equivalent or exceeding the Laplace pressure) needs to be supplied by a velocity gradient. The average velocity
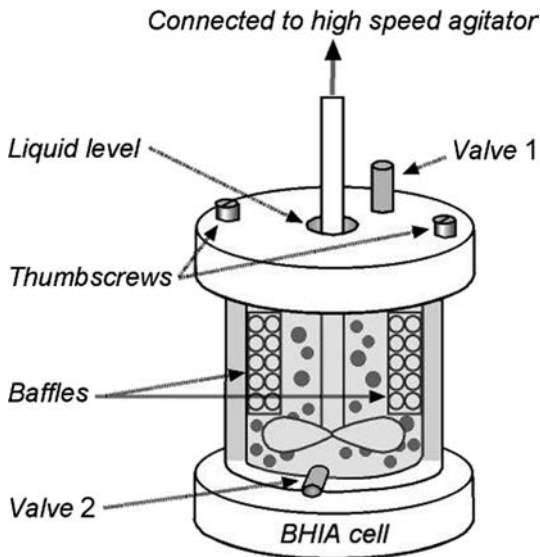
gradient may vary according to the type of stirring and the size and shape of the vessel, and it may be noted that local velocity gradients can be higher than the average which results in local elongations of flow and are more effective in disrupting bubbles than simple shear. Generally, it is very difficult to generate bubbles smaller than a few tenths of a millimeter in diameter unless very high-intensity agitation (which causes cavitation effects) is used. Most studies show that the bubble size can be reduced by increasing the beating speed (velocity gradient), but this is not always the case. In some mechanical processes carried out at a constant beating speed, the amount of foam has been found to decrease again after a certain time. This may be explained by a non-desirable heating up of the foam.

During the mechanical whipping or rotation methods, the disrupting stress can be shear, normal or inertial depending on the energy input of the whipping head, which can cause several different types of disruption processes as the bubbles migrate through the shear field. For a successful bubble generation step, a sufficient quantity of surfactant needs to be rapidly supplied to the gas/liquid interface to create a surface tension gradient (to ensure a high Gibbs elasticity) which acts to stabilize the fresh bubbles. Since shearing is often a continuous process and the rates of bubble formation may exceed the capacity of surfactant to maintain equilibrium adsorption conditions, after a period of time bubble coalescence may begin to occur due to starvation of the interface. High surface tension gradients are essential for foam stability, since the individual foam films must resist both external pressure within the Plateau borders and pressure oscillations due to turbulence. In many industrial systems, several different types of surfactants and polymers are present, and the competitive rate of diffusion of these different types of surfactants needs to be taken into consideration. Adding a suitable polymer (to the surfactant solution) which substantially increases the liquid viscosity at low shear stress can also prevent bubble coalescence.
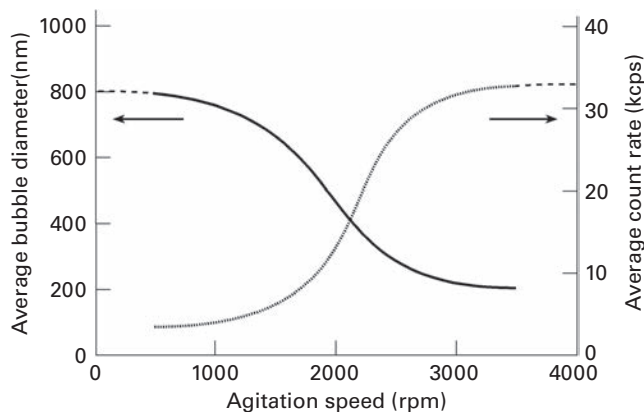
5.5.1   High-intensity agitation (cavitation)

Cavitation is one of the widely used methods of generating nano-bubbles, and there are several different methods of producing this event. It may be classified as (a) hydrodynamic cavitation by fluid flow, (b) acoustic cavitation by acoustic energy, (c) optical cavitation by using photons from a laser and (d) particle cavitation, induced by elementary particles. In 2012, Wu and coworkers (4) designed a baffled, high-intensity agitator which is shown in Fig. 5.5, and successfully produced submicron-sized bubbles by hydrodynamic cavitation. Sodium dodecyl sulfate, DowFroth 250 (a nonionic commercial polyethylene surfactant), a dilute electrolyte solution and sea water were used in these systems. The bubble size and charge on the bubbles were measured using a ZetaPALS instrument (Brookhaven Instruments Corporation).

Following an increase in agitation speed, the bubble size was reduced (as shown in Fig. 5.6), and at high speeds (in the region of 3500 rpm) bubbles less than 200 nm were produced which had a relatively narrow size range. It was reported that the temperature had little influence on the bubble size up to 50°C. The surfactant-stabilized bubbles were reported to have a lifetimes of over 24 hours, but for bubbles generated in sea water and

Fig. 5.5 A schematic diagram of the baffled high-intensity agitation cell; valves 1 and 2 are used to take samples for bubble size distribution and zeta potential measurements. From ref (4).
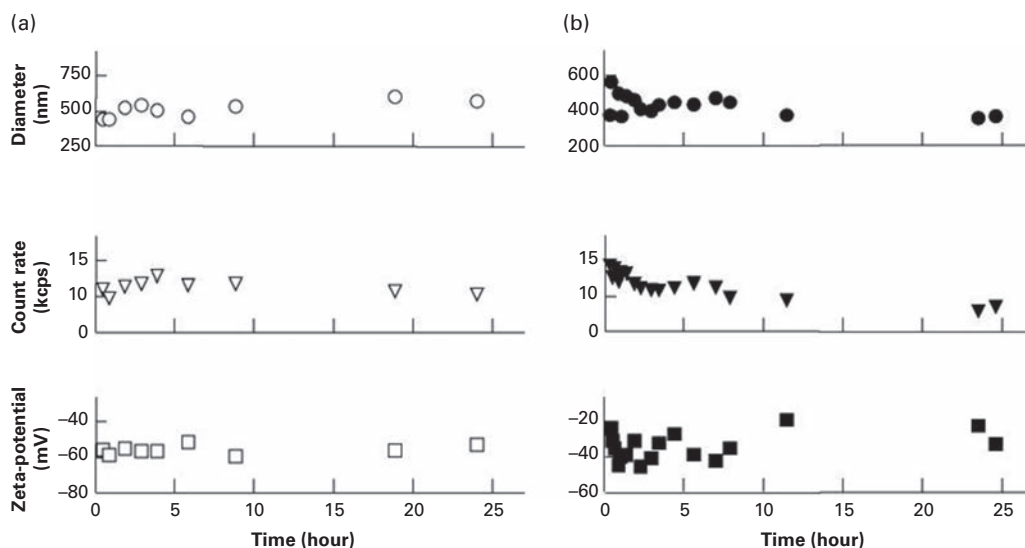

Fig. 5.6 Effect of agitation speed on generation of submicron size bubbles in SDS (1 mM) and KCl (1 mM) solutions in pH 6.0 The agitation time was fixed at 30 min. From ref (4).

in a solution of weak electrolyte, the stability was lower. The charge on the bubble was found to be in the region of –60 mV and was pH dependent. Some of the results with respect to bubble stability, zeta potential and bubble count rates are shown in Fig. 5.7. The bubbles were found to be charge-stabilized.

5.5.2 Rotary stirring in food processing

In recent years considerable research efforts have been invested in foam process engineering, and several different types of high-speed rotary mixers, stirrers and
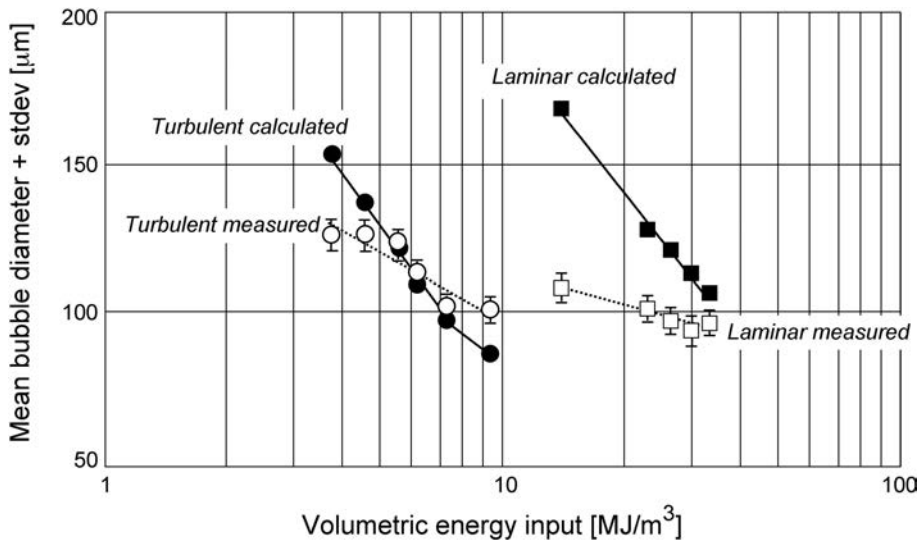
Fig. 5.7   Stability and charge of submicron size bubbles (a) generated in 1 mM SDS and 1 mM KCl solution at pH 6.0 at 2000 rpm for 30 minutes and (b) in 0.1 mM DF 250 (a nonionic frother Dowfax) and 1 mM KCl solution at pH 7.0 at 2000 rpm for 30 min. From ref (4).

similar blade-driven mixing vessels have been designed to achieve more effective entrainment of gas, with the aim of producing foams with smaller bubble size and narrower distribution. These methods are widely used for commercial processes, such as in the preparation of food foams, foam-coated fabric and polymeric carpet-backing foams. In food processing, it is generally accepted that small bubbles give improved texture and flow characteristics with a creamier mouthfeel and prolonged shelf life. However, most of these studies on whipping and shearing are empirically based, and very few studies have been carried out under well-defined hydrodynamic shearing conditions. In fact, there are only a few papers dealing with continuous whipping processes which relate the process conditions to the foam microstructure.

In most rotor–stator units, an increase in power input causes a transition to occur from laminar to turbulent flow and in the laminar flow field, it is assumed that the shear stress mainly contributes to the deformation and break-up of the bubbles. From these experimental studies it has been generally accepted that there are several process parameters which can influence the bubble size distribution and microstructure of food foams, for example, the impact of residence time on the dispersing flow field, the rotational velocity of the whipping tool, the overrun (gas fraction in foam) and the back pressure. A series of early interesting experiments were carried out by Hirst and Prudhomme (5) using a commercially produced rotary mixer designed by Oakes Corp. (Islip, NY), with blades attached to both sides of the rotor. The gas–liquid mixtures were pumped into the center of the vessel and shearing occurred in gaps between the blades. Bubble sizes were measured and related to the processing
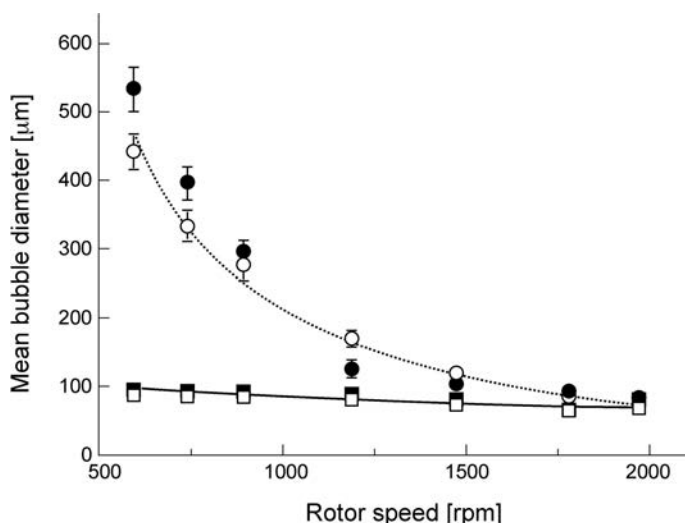
Fig. 5.8 Measured and theoretical calculated maximum bubble diameter versus volumetric energy input under laminar and turbulent flow conditions with residence time of 43 seconds and over-run 300%. Whey protein isolate was used as the foaming agent. From ref (6).

conditions. The influence of the fluid viscosity during shearing was also studied and it was found that an increase in rotation speed (shear rate) decreased bubble size irrespective of the viscosity of the fluid, and it was also found possible to generate fine-scale foams using this equipment.

Later, Hanselmann and Windhab (6) derived theoretical equations from the power characteristics of a rotor-stator whipping device. The rheological features of the foam and the laminar and turbulent whipping flow conditions were used to estimate the maximum bubble diameter. They used a dispersion containing whey protein isolate (as a foaming agent) and a guar gum additive to change the viscosity of the dispersion. Overrun (gas-intake) and bubble size distribution were measured. The results are shown in Fig. 5.8, where it can be seen that reasonable agreement exists between the calculated and experimental bubble diameters under both laminar and turbulent flow conditions.

From the study, it was established that the mechanical energy input had the most important influence on the processing, and this parameter could be related to the rotor speed, the viscosity and the residence time. The dispersion of gas was shown to be superior in the turbulent flow field, moderate in the transition region and poor in laminar flow for the same low viscosity system. An improvement in gas dispersion in the laminar flow field was also achieved with a more highly viscous fluid, and this consequently resulted in an increase in the mechanical energy input. The relationship between the mean bubble size and the rotor speed at different residence times with different viscosity dispersions is shown in Fig. 5.9.

Another important conclusion from these studies was that the rotor speed alone cannot be taken as a reference in foam generation. Depending on the foaming characteristics of the system, the flow field (at the same rotor speed) can cause differences in the degree of gas dispersion, thus also causing differences in the resulting foam quality and stability.
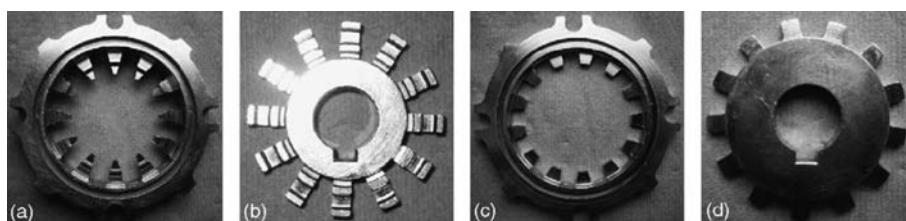
Fig. 5.9 The mean bubble diameter versus rotor speed at different residence times and an overrun (gas intake) of 380%. Protein isolate additives (Bipro tv) were used as a foaming agent and guar gum was used to modify the viscosity. The different residence times in the mixer are as follows; ● 15s for Bipro tv; ○ 73 s for Bipro tv; 73s □ 73s for Bipro tv + guar and ■ 37 s for Bipro tv + guar. From ref (6).

It was also reported that the absolute degree of gas dispersion was strongly dependent on the viscosity, but the residence time of the impellor in the blender also has an influence on bubble size in the laminar flow field for low viscosity liquids. In order to achieve improved foam quality, it was suggested in this study that the relationship between bubble size and process conditions needed to be carefully investigated in other types of rotor mixers.

In a further study by Muller-Fischer and Windhab in 2005 (7), whipping devices with adjustable rotor–stator geometry were used to study the influence of several different parameters on the mean bubble size distribution and microstructure of the foam. These parameters included the residence time in the dispersing flow field, the rotational velocity of whipping tool, the overrun (gas fraction in foam) and the pressure produced by the whipping head. These workers carried out experiments with a model system that used a milk protein and a guar gum, and it was concluded that the pressure applied to the whipping head had the governing impact on the bubble size, but increases in overrun caused bubble coalescence. The application of back-pressure on the whipping head resulted in the dispersion of higher gas fractions, but an increase in viscosity or velocity caused problems due to heating effects. Several different types of rotor–stator whipping head geometry (as illustrated in Fig. 5.10) were used in the experiments.

Foaming at reduced pressure (vacuum conditions) was suggested as an alternative to the traditional back-pressure foaming procedures. Using such vacuum methods, it was found that bubble expansion was avoided when the mixture is subject to ambient pressure which usually occurred in back-pressure foaming. However, partial vacuum whipping resulted in increased bubble re-coalescence.
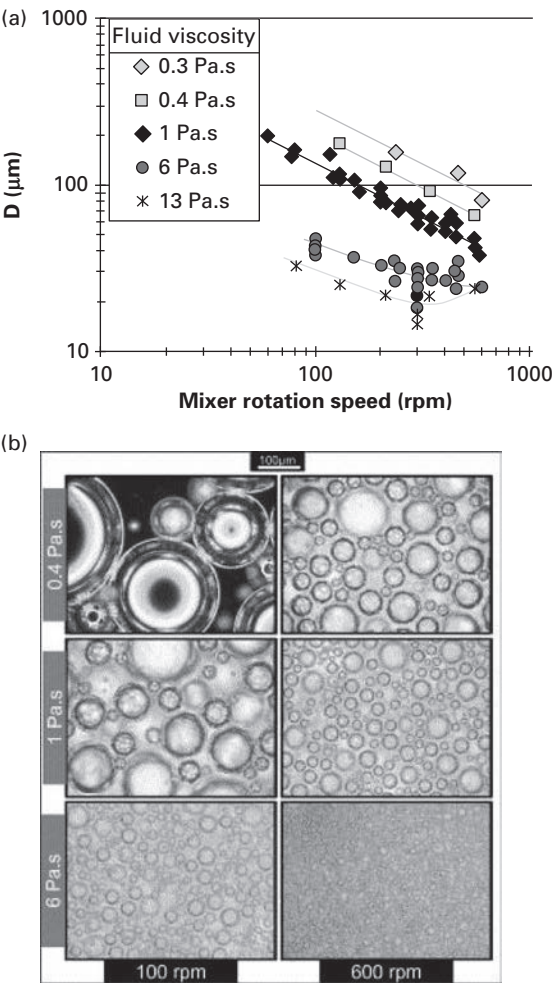
Fig. 5.10 Different types of whipping geometries: (a), (b), (c) and (d). From ref (7).

The effect of processing conditions (pressure, flow rates, whipping rotation speed) and formulation properties on the bubble size of food foams was studied by Balerin and coworkers in 2007 (8). In this study, model fluids were formulated which were composed of dilute glucose syrup to adjust the viscosity and whey protein which consisted of mainly β-lactoglobulin and α-lactalbumin. Solutions with viscosities in the range of 0.4–13 Pas were foamed in a fully instrumented pilot scale line that enabled the process to be accurately monitored, and the bubble size was determined under pressure at the exit of the mixer. Heating effects were also measured and were shown to be an important influence during the foaming of the high viscosity solutions. It was concluded that the viscosity and rotation speed of the whipping head had the most important influence on the foam morphology, but it was also found that the fluid viscosity in the whipping head was reduced due to local heating. The results presented in Fig. 5.11(a) show the relationship between bubble size and rotation speed. For each viscosity, the bubble diameter decreased as the mixer rotation speed increased, but this did not occur to the same extent for all viscosities, as illustrated in Fig. 5.11(b), which depicts foams formed from a solution of three different viscosities at two different mixing rates. The reduction in bubble diameter is most pronounced for low viscosity fluids, but for high viscosity fluids and higher rotation rates, the bubble size tended to level off, and it was suggested that this was caused by local heating effects.
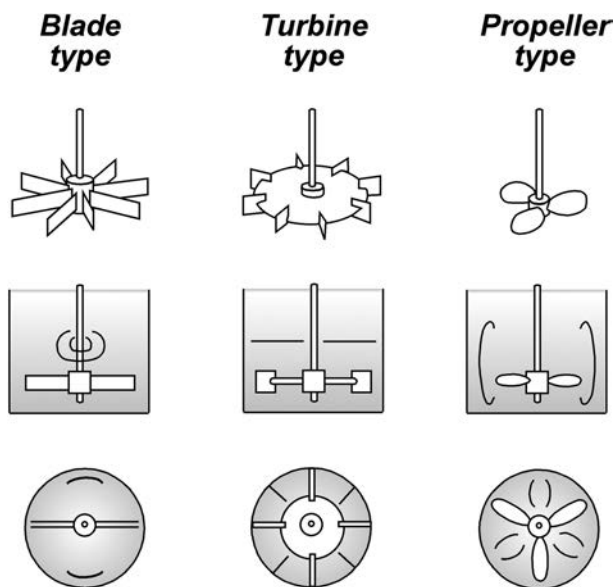
5.5.3 Rotary stirring in mineral processing

Froth flotation is a vast industry in which bubbles and foams are generated in the presence of dispersed particles and surfactant (collector) and froth stabilizers. Today, many different types of flotation machines are used throughout the world. Strong agitation is needed where fairly dense millimeter-sized particles need to be effectively dispersed and air bubbles generated in tanks. Different types of common agitators, corresponding to different types of fluid flow patterns, are shown in Fig. 5.12. The blade-type impellor produces a rotary action in a circular direction, the turbine-type impellor gives rise to flow in a radial direction and the propeller-type impellor produces up-and-down convective circulation flow in an axial direction. Most of the machines and cells have been designed by different manufacturers, and each machine has its own characteristics. While the mechanical design differs from cell to cell, the internal hydrodynamics may be classified into one of two possible flow patterns, as indicated in Fig. 5.13.

Fig. 5.11 (a) Evaluation of bubble mean diameter D, at different mixer rotation speed for fluids with different viscosities and (b) microscopic pictures of foams obtained by whipping of three different model fluids (with different viscosities) at two different rotation speeds (gas content 50%). From ref (8).
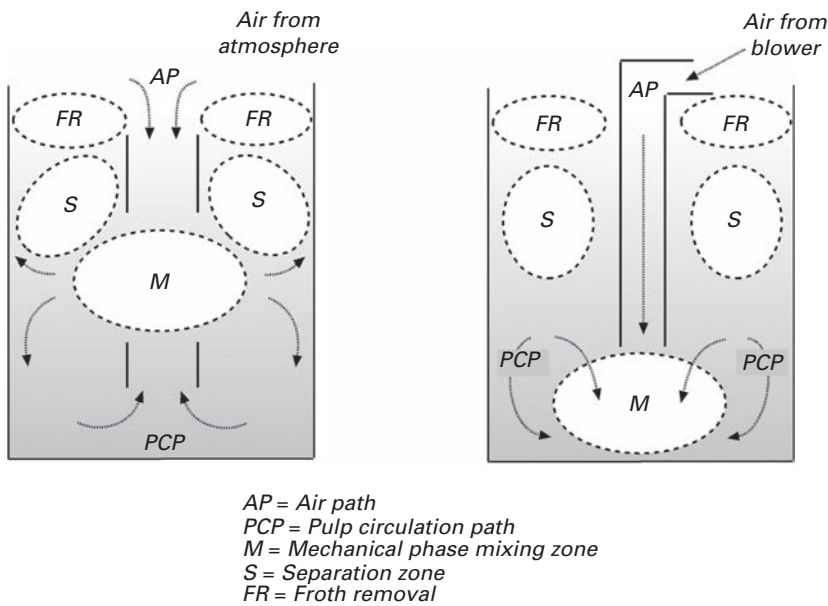
The self-induced cell has a mechanical mixing zone in the central tank region, and when the rotating impeller depresses the interface entrainment of air occurs. This is followed by bubbles circulating in the cell that impact and capture the more valuable mineral particles. In the separation zone, which is located in the upper region of the cell, the hydrophobic particles remain attached to the bubbles whereas the hydrophilic particles sink to the lower region of the cell. In the supercharged-type mechanical flotation machine, air is introduced from an external blower and the mechanical separation zone is in the base of the cell. Most machines are open-flow type which ensure high throughput, and are also easy and inexpensive to maintain. In recent years, several modifications have improved the impellor system and the tank geometry, thus increasing process efficiency and throughput.

Fig. 5.12   Relationship between the impellor and the resultant fluid flow pattern. From ref (9).

(a) Self-induced type cell   (b) Supercharged type cell

AP = Air path
PCP = Pulp circulation path
M = Mechanical phase mixing zone
S = Separation zone
FR = Froth removal

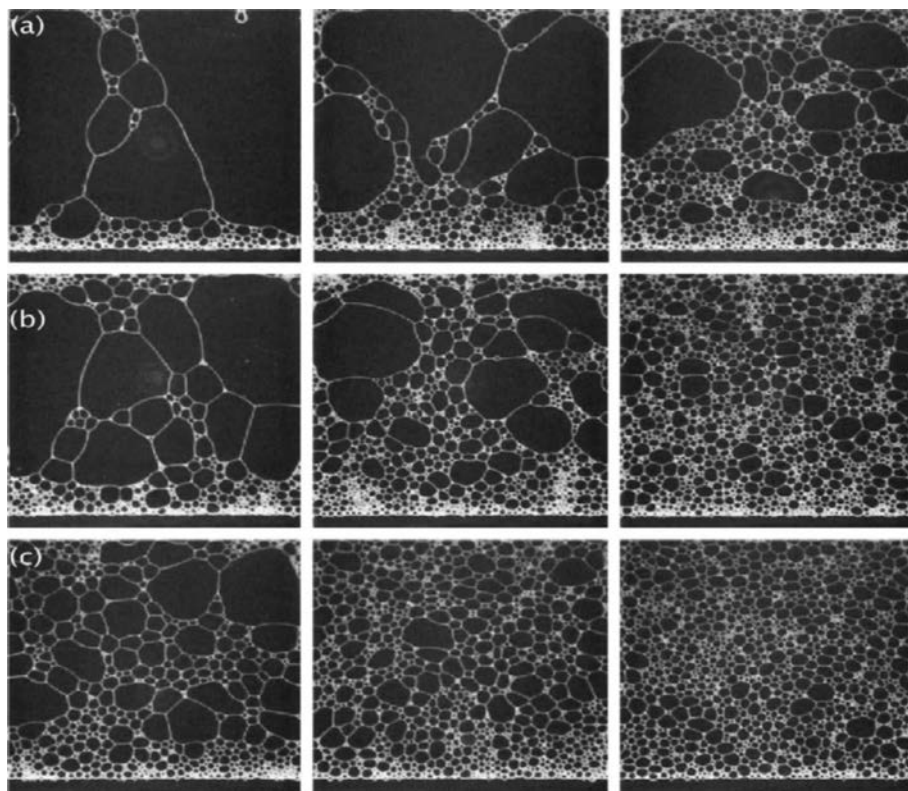**Fig. 5.13**   The hydrodynamics of mechanical flotation machines. From ref (9).

5.5.4   Shaking or successive flipping

To compare the foaming behavior of different surfactants, many different types of simple laboratory tests have been developed, such as shaking or flipping a known volume of solution for a predetermined time period in a closed container. The handshaking test is simple and quick and usually carried out in narrow tubes. However, low foaming surfactants often give poor reproducibility due to wall effects, and bubble shapes which influence foam heights and are be difficult to define in these types of tests, and generally, accurate measurements of foam stability cannot be easily achieved. However, in 2006 and 2007, experimental studies by Caps and coworkers (10, 11) were carried out in which 2D foams were generated by a precise and reproducible technique. This is based on flipping using a specially designed cell, known as the Hele-Shaw (H-S) cell, which is constructed from two plastic or glass plates (13 cm × 13 cm) separated by a thin liquid film (0.3 cm) into which the surfactant solution is introduced.
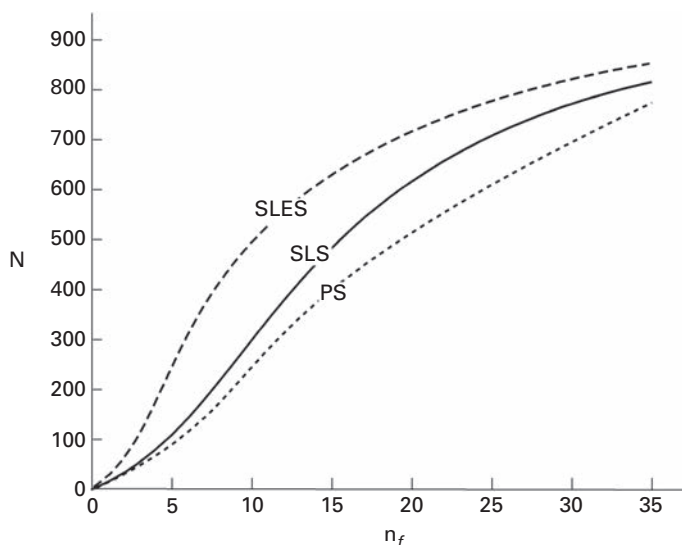
The cell is initially partially filled with a surfactant solution (6 cm^3) and attached to a horizontal rod that is rotated by a motor. It is flipped (usually at a rate of two rotations per second), and between each upside-down flip, the H-S cell is left to rest for 10 s (which can be varied slightly, depending on the surfactant solution). This enables the foam to drain, and topological rearrangements of the structure occur during this process. During the flipping motion, an intermittent wetting of the cell occurs and gravity causes downward motion of the liquid which flows through Plateau borders and dries the top of the foam, while the bottom remains wet due to capillary forces. Clusters of the larger bubbles are produced in different places in the cell during the flipping process, but eventually the larger bubbles disintegrate and gradually the mean bubble size gets smaller. Eventually, the foam becomes homogeneous, consisting mostly of nearly hexagonal bubbles in agreement with Plateau's rules. As the number of flips increases, an increasing number of bubbles which compose the foam, are formed. The maximum number of bubbles produced usually depends on the amount of liquid in the cell.

This foam generation process is reproducible and extremely sensitive to the type and concentration of surfactant in the solution. The remarkable feature of the system is the fast decrease of the standard deviation of the bubble size during the successive flips. Pictures of the cell are taken automatically after each flip, and an algorithm was developed to recognize all bubbles and measure the sizes, positions and of their center of mass and shapes. In Fig. 5.14, a series of typical images of the foam produced from three different surfactants at different stages of generation (after 1, 15 and 30 flips) are shown. During the flips, the number (n_f) of bubbles increases and tends to take an asymptotic value which depends on the initial water content. In Fig. 5.15, the data relate the evolution of bubbles to the number of flips of the cells for three different surfactants. The curves were shown to fit a theoretical model. The technique enables homogeneous 2D foams from different surfactant systems to be easily characterized and compared. The method has been shown to be useful for studying and characterizing the generation steps and the structures of foams.

Fig. 5.14 Typical images of the foam generated in the Hele-Shaw cell after $n_f = 1$, 15 and 30 flips. Three different surfactant systems used in the experiments are (a) paraffin sulfonate (PS), (b) sodium lauryl sulfate (SLS) and (c) sodium laureth sulfate (SLES). From ref (10).

Fig. 5.15 The evolution of the number (N) of bubbles composing the foam as a function of the number of n_f of flips. Three surfactants are paraffin sulfonate (PS), sodium lauryl sulfate (SLS), and sodium laureth sulfate (SLES). The continuous curves are fit according to an evolution law that which was derived from a kinetic model for the splitting process. From ref (10).
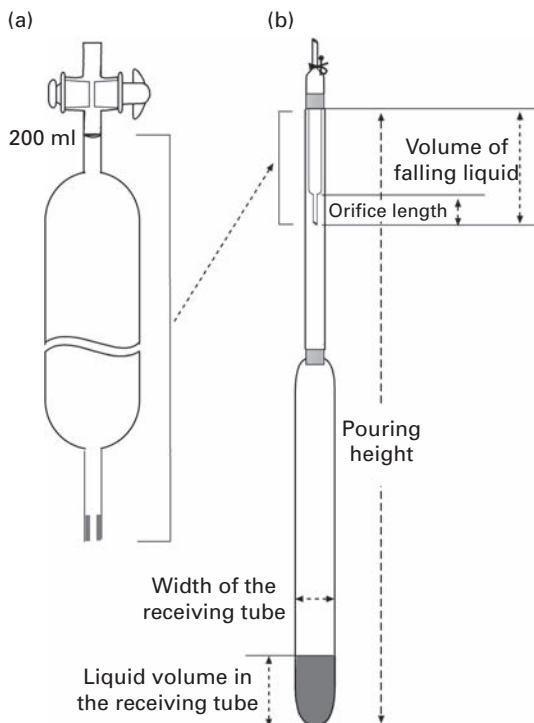
5.5.5   Pouring and plunging jet methods

This method is based on pouring a given amount of foaming solution (from a pre-determined height) into an empty vessel. This test enables both the generation and the rate of decay of the foam to be monitored. The advantage of this method is that it is capable of producing foams at fairly low surfactant concentrations, which is more difficult to generate using sparging methods. The test mimics the foaming behavior in many different types of industrial filling processes with an example being the filling of containers with soft drinks using high-speed jets. Turbulent flow occurs as the jet strikes the interface of the liquid (which is already in the vessel) and causes air entrainment and foaming. The generation process can be carried out as a static or as a continuous process. The continuous plunging jet method is fairly novel and gives additional information to the static test.

5.5.5.1   Static plunging jet

The static test is relatively simple and has been adapted from the traditional standard test method for the beverage industry for pouring (see the Ross–Miles test method ASTM D1173-53 in Chapter 11). A typical set-up constructed by Wallin (12) in 2005 is shown in Fig. 5.16.
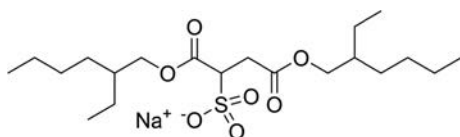

Fig. 5.16   The plunging jet method, based on the Ross–Miles test, used to generate foam in filling beverages. From ref (12).

This apparatus enabled several different parameters (volume of falling liquid, pouring height, orifice diameter and width of the receiving tube) to be varied and their influence on the foam height to be quantified. From detailed studies, the pouring height was found to have the most important influence on the volume of foam initially generated, but also the foam volume was found to increase with the volume of falling liquid. An increase of the orifice diameter of the pipette and also an increase in the orifice length caused an increase in foam volume. Some theoretical aspects of the generation process were considered and an attempt was made to quantify the kinetic energy involved as the jet of liquid strikes the surface of the foam. The process was also discussed in terms of the liquid jet penetrating into the interface, which caused turbulent flow within the liquid column entrapping air.
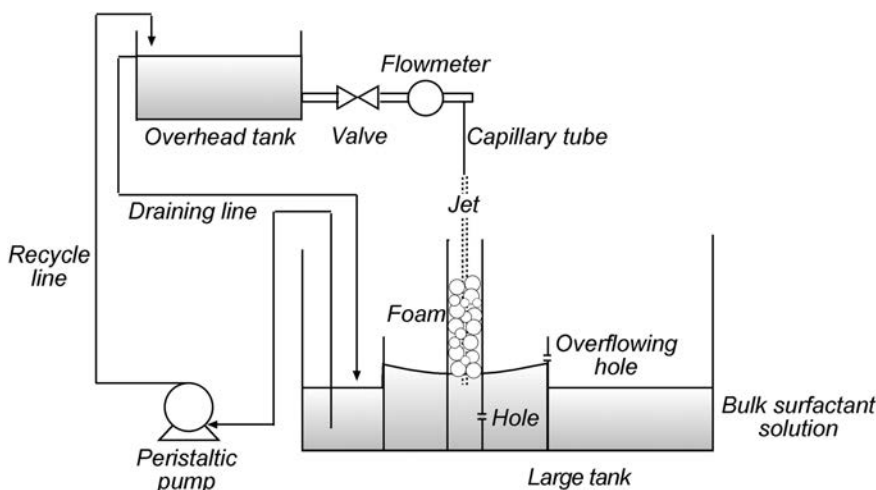
5.5.5.2   Continuous plunging jet

The continuous process is more difficult to construct but frequently occurs in many industrial processes such as overflows in settling tanks and reactors and can be also observed in nature, such as waterfalls. Early studies of the plunging jet test established that the size of the vessels and height the solution falls are important parameters that influence foam generation. Many variations of the method have been introduced by the industry for different applications, such as mixing liquids with gases in reactors. An interesting investigation was carried out in 2005 at Imperial College, London (13), using the continuous plunging jet method to evaluate the foaming behavior of a solution containing a versatile anionic surfactant sodium bis-2 (ethyl-hexyl) sulfosuccinate (commonly known as AOT) which has a polar tail and polar head group and can form normal and reverse micelles in solution (see Fig. 5.17 for molecular structure).

The plunging jet equipment was designed with a large overhead tank from which a jet of foaming liquid was allowed to fall into a cylindrical column. After the generation of foam, the residual liquid could be pumped back into the overhead tank again so that the surfactant solution could be continuously circulated. The drainage pipe in the overhead tank ensures a constant hydrostatic head of liquid, so that the jet pressure remains constant. As the liquid jet impacted the surface, entrainment of air occurred, generating foam in the cylinder. Both static (without recirculation of liquid) and continuous (with circulation) experiments were carried out and the methods were found to be flexible enabling key processing variables, such as falling height and size of the column, to be changed. The apparatus is shown in Fig. 5.18.
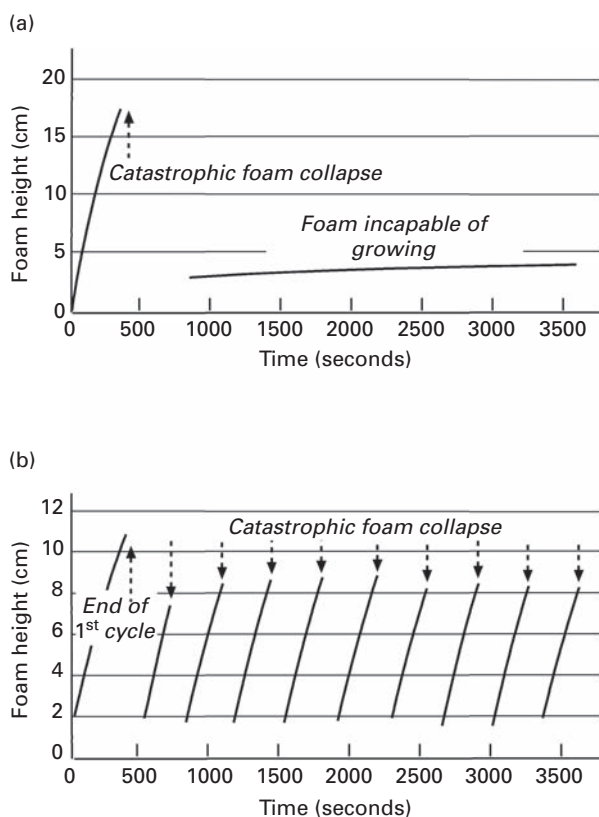

Fig. 5.17   The anionic surfactant sodium bis-2 (ethyl-hexyl) sulfosuccinate.

Fig. 5.18   Apparatus for producing foam by the continuous plunging jet method. From ref (13).

Initially, in the static tests, the influence of several experimental variables was investigated including falling height, pool depth, surfactant concentration (which was usually below the CMC), jet flow rate and column diameter. From the experiments, it was reported that the pool depth had no influence on the foam height (in the low surfactant regions) but, as the AOT concentration increased, the amount of foam generated increased. At low falling heights, foaming increases with height, but after a given height it was found to remain reasonably constant. At low jet speeds, the amount of foam showed no significant change, as the falling heights were increased. Only at high jet speeds did the degree of foaming increase with increased foaming height. It was further reported that the pool depth had no influence on foaming. After reaching a maximum foam height, in the case of foams generated by the continuous plunging jet test at high surfactant concentrations, it was found that a catastrophic (i.e. near total) collapse of foam occurred. However, the foam then re-generated itself and this process appeared to consist of three steps: generation, collapse and regeneration. However, it was found that the height at which the foam regenerated itself was always less than the first initial foam height. This situation is shown in Fig. 5.19.

Usually, the maximum volume of foam produced (just before collapse occurs) was taken as a measure of foam generation. The collapse process appeared to be initiated by the bursting of a single foam film which caused a catastrophic avalanche-type foam collapse, propagating from the top to the bottom of the foam layer. This cyclical instability phenomenon was found to occur within a critical surfactant concentration range. The results were reproducible and it was possible to characterize the process according to well-defined collapse frequencies. From this study, the dynamic foaming behavior could be defined into four distinct types or operating regimes according to the surfactant concentration. At low AOT concentrations, bubbles were observed at the surface but were
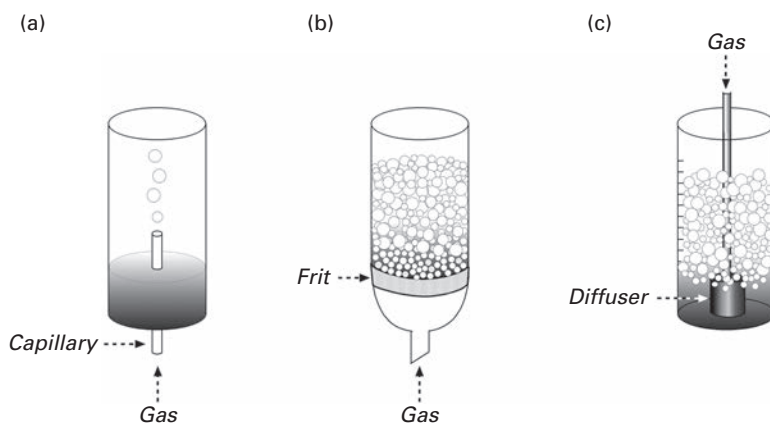
Fig. 5.19   (a) Successive growth and collapse behavior at a low AOT concentration below the CMC at 0.0.031 g/l at jet flow rate of 172 m/min using a 5.4 cm column diameter and (b) cyclic unstable foam behavior at AOT 0.125 g/l at jet flow rate of 172 m/min using a 5.4 cm column diameter. From ref (13).

unstable and burst rapidly as the liquid jet fell continuously on the pool. In this region it could be suggested that the concentration of surfactant was too low to stabilize the foam. However, upon increasing the concentration of AOT, cyclic behavior was observed, which was of greater interest. In this regime, foam grows and collapses at regular frequencies, and the height at which the foam grows is always less than the initial height. Finally, at fairly high surfactant concentration (about 40% of the CMC concentration), a stable foam regime was observed in which the foam column reached a maximum height and thereafter remained stable. It was found that the rate of generation of foam was equal to the rate of foam collapse and volume remained at a maximum irrespective of jet flow rates.

5.6   Growing bubbles from single orifices, frits and gas injection

Foams may also be generated by introducing gas into a liquid using a single orifice, fritted filter or gas diffuser, as shown in Fig. 5.20.

Fig. 5.20   Aeration methods for generation of foams: (a) single capillary, (b) fritted filter or (c) gas diffuser.

The advantages of the single bubbles, released from a capillary in the static regime, are that bubbles and foams that are almost monodisperse, with each bubble released having the same size. This enables model foams and bubble rafts to be constructed that resemble hexagonal close-packed monodispersed spheres. The method is also of particular interest because it enables measurement of dynamic surface tension by the maximum bubble pressure method (Chapter 1) to be carried out, which is particularly relevant for foam generation. Bubbles produced from a frit are usually in a wide size range depending on the frit type. Gas injection also produces a wide range of bubble sizes.

5.6.1   Detachment of a bubble from single orifices

Under constant gas flow rate conditions which are sufficiently slow to be in the quasi-static regime, Dickenson (14) suggested that the size of bubbles (produced at an orifice) may be roughly estimated theoretically by equating the buoyancy force (F_b) with the force associated with surface tension (F_s) acting on the emerging bubble, where

$$F_b = (4\pi/3)(r_b^3 \rho \, g) \tag{5.3}$$

and

$$F_s = 2 \, \pi \, r_o \gamma \tag{5.4}$$

In these equations, r_b and r_o are the radii of the bubble and orifice, respectively, γ is the surface tension and ρ is the specific gravity of the liquid. Under idealized conditions, an estimate of the radius of the emerging bubble may be obtained by assuming these two forces are equal at the moment of bubble release from the orifice, so that

$$r_b = (3 \, \gamma \, r_o/2 \, \rho \, g)^{1/3} \tag{5.5}$$

However, in practice, since the dynamic surface tension of the growing bubble is higher than the equilibrium surface tension, depending on the wetting conditions, the contact base may spread. Numerous detailed experimental studies have been reported dealing with the influence of interfacial tension, cleanliness of the surface and gas flow rate, etc., on the formation, growth and detachment of a bubble from an orifice. The key factor that influences the bubble volume is the so-called adhesion tension, $\gamma \cos \Theta$, where Θ is the contact angle. Lin et al. (15, 16) have recently demonstrated that for a single liquid system, the contact angle of the liquid on the solid plays a key role in controlling (a) the spreading of the contact base, (b) the bubble attachment to the surface and (c) the bubble closing process which occurs immediately prior to detachment. In this study, experiments were carried out on flat steel horizontal and inclined plates containing holes (produced by a laser beam). The surface energy of the plate was modified by plasma deposition of an ultrathin layer of different polymers, enabling different contact angles to be investigated. With a hydrophobic surface, a bubble which was significantly greater than the size of the hole developed (due to the non-wetting nature of the surface). In the case of hydrophilic surface (low contact angle), no contact base was observed, but the size of the hole had a critical influence on the size of the bubble. It was also found necessary to distinguish between the equilibrium contact angle Θ (used to characterize the surface) and the dynamic contact angle β, observed during bubble growth. Figure 5.21 shows a range of bubble formation profiles for different orifice plates (after surface treatment) giving different equilibrium contact angles.

Fig. 5.21 Bubble formation profiles for the various orifice plates with different equilibrium contact angles (Θ). The dynamic contact angle β changes with time of bubble development. Top: Contact angle $< 45°$; contact base diameter $= 0.55$ mm; bubble volume $= 0.011$ ml. Middle: Contact angle $= 80.5°$; contact base diameter $= 3.0$ mm; bubble volume $= 0.05$ ml. Bottom: Contact angle $= 99.7°$; contact base diameter $= 4.8$ mm; bubble volume $= 0.101$ ml. From ref (15).
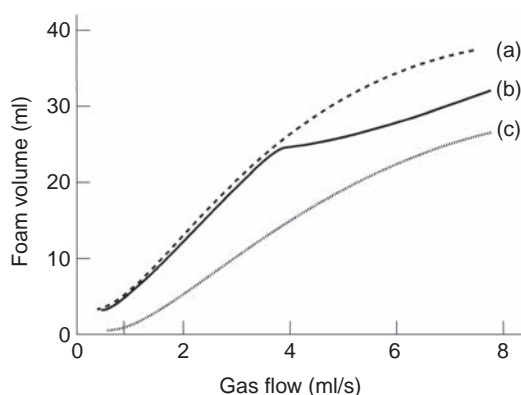
As the bubble detaches from the orifice, the dimensions of the bubble will dictate the velocity of rise. In addition, as the bubble rises, a redistribution of surfactant on the bubble surface results in a reduced concentration at the upper surface with the polar base having a higher concentration than the equilibrium value which plays an important role in the stability of the foam. Additionally, as the bubble arrives at the interface, a thin film is produced on top of the bubble. The lifetime of this thin film and the probability of producing foam depend on numerous factors such as the surfactant concentration, drainage rate, surface tension gradient, surface diffusion, external disturbances, etc. Larger bubbles and higher production rates can be obtained by using greater gas flow rates, such that the viscous forces play a role in the bubble formation and surface tension becomes less important. Even larger bubbles can be obtained by placing the nozzle under a plate to reduce its effective buoyancy and the bubble size can be controlled by changing the angle of the plate.

As the bubble stream rises a foam layer is produced at the surface of the column. This can produce monodispersed samples if the gas flow rate is small and constant (e.g. by using an air pump), but if the flow is increased, the bubble emission process bifurcates to produce a variety of bubble sizes. This is the first step toward chaotic behavior that occurs at high flow rates and causes polydispersed foams. In fact, bubble production by use of a single nozzle has been used as a very simple demonstration of chaotic dynamics (17). The transition from regular to irregular flow is mostly determined by the flow rates, and at slow flow rates the bubbles are periodic and widely spaced. At increasing flow rates the spacing between bubbles is reduced and the creation of each individual bubble can be influenced by the presence of the previously created bubble. As the flow rate is increased the spacing decreases and the formation of each bubble may have an influence on the presence of the previous one. Bubbling modes have been observed and the different process regimes characterized as periodic, periodic doubled and chaotic. Period doubling was found to lead to chaotic behavior.

5.6.2   Growing bubbles using frits

The process of injecting a gas at a constant flow rate into a liquid through fine orifices in a porous disc is known as "sparging" and is frequently used in industry and in the laboratory. As the bubble stream rises, a foam layer is produced at the surface of the column. The flow rate, the pore size of the frit, the vessel size and shape and also the quantity of solution are important parameters that determine the amount of foam produced. On a small scale, this method is widely used in academic studies by means of controlled bubbling. It is advantageous in that it can distinguish between dynamic and static foaming regimes which are dependent on gas flow rates. At low gas flow rates, the volume of foam generated is directly related to the gas flow rate, but at high flow rates, this relationship breaks down since the surface-active foamer does not have sufficient time to reach equilibrium adsorption coverage on the bubble surface causing starvation and coalescence. In Fig. 5.22, the results are shown from sparging experiments carried out in a cylindrical column to compare the foaming performance of fresh and aged surface-active nano-sized silica particles dispersed in water and

Fig. 5.22 The foam volume versus gas flow rates for foams stabilized by partially hydrophobic silica nanoparticles: (a) no salt (6.4s); (b) 0.1 M NaCl, fresh; and (c) 0.01 M NaCl, aged 17 weeks. From ref (18).
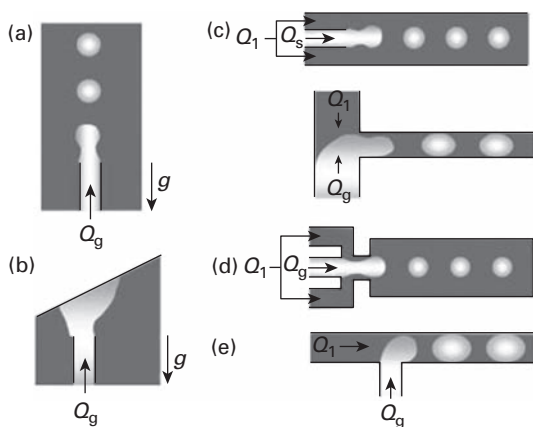
weak electrolyte solution. Each system shows a liner relationship between the foam volume and the gas flow rate in the low gas flow regions, but at gas flow rates greater than 4 ml/s this relationship breaks down particularly in the case of the 0.1 NaCl, fresh system, due to insufficient particles reaching the bubble interface, resulting in some coalescence. In this study it was shown that the partially hydrophobic silica nanoparticles acted as weaker surface active foamers on aging.

5.6.3 Co-injection

Co-injection is the process of simultaneous injection of a gas and foaming solution into a porous material or injection tube. The size of packing in the porous material plays an important role in controlling the type of foam. The method is commonly used in the cosmetic industry for generating shaving creams, and Gillette uses specialized formulations consisting mainly of an aqueous solution of mixed surfactants (stearic acid and triethanolamine). This solution is supersaturated with hydrocarbon gases (isobutene, propane and butane) and, upon releasing the contents from a container, the gases are released from the solution, producing bubbles stabilized by the surfactants. Many different types of devices to generate fire-fighting foams also employ injection strategies.

5.6.4 Monodispersed bubbles and microfluidic foams

Over the past 10 years, there has been a considerable interest in producing small agglomerates of monodispersed, micron-sized bubbles and microfluidic foams. Microfluidics is the science and technology of systems that process or manipulate small amounts of fluids through restricting small channels with sizes in the range from tens to hundreds of microns. Discrete microfluidics employs droplets, bubbles or foams, with applications on the larger than micron scale. Microfluidic devices have shown to
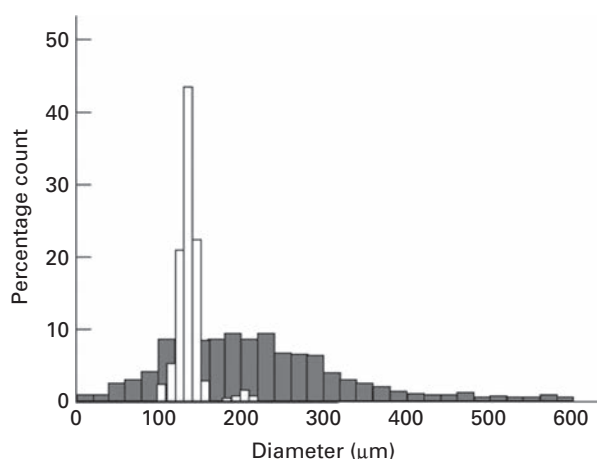
Fig. 5.23   Preparation of small monodispersed bubbles by (a) traditional bubble through nozzle, (b) bubbling under an inclined surface to generate large bubble, (c) mini/microfluidic techniques in which the liquid and gas are injected at constant flow rates (Ql and Qg respectively) causing the formation of a thin gas thread which breaks up into monodispersed bubbles. One generally makes a distinction between (c) symmetric and asymmetric confined co-flow (d) flow-focusing and (d) cross-flow (or T-junction). From ref (19).
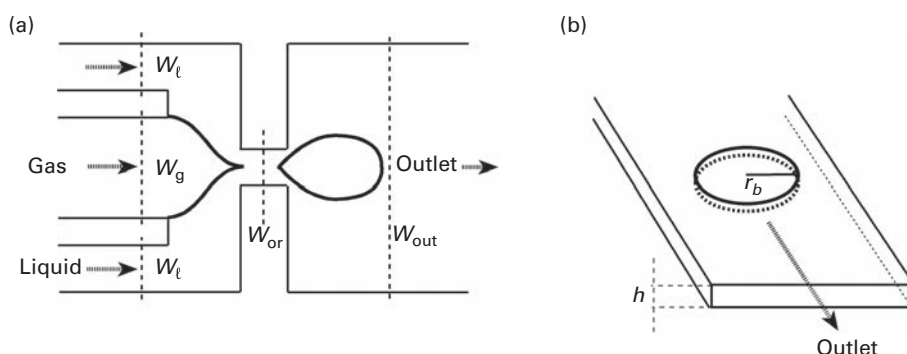
have a wide range of novel applications associated with high throughput screening, protein crystallization and ultrasonic contrasting.

Several different types of microfluidic systems have been developed and most have been based on the co-injection of gas and liquid simultaneously at constant pressure or constant flow rate into narrow hydrophilic channels. The gaseous phase fragments into small monodispersed bubbles under laminar flow conditions. Depending on the geometry of the channels, one can distinguish between different types of systems which may be classified as confined co-flow, flow-focusing or cross-flow. In Fig. 5.23, three different types of systems are shown (c, d, e) which are compared with the traditional methods of preparing monodispersed bubbles (a, b). In the generation of microfluidic foams, the gaseous phase break-up process is characterized by three distinct regimes which can be classified as (a) squeezing, (b) dripping and (c) jetting. Essentially, the bubble size is controlled by the magnitude of several physical parameters (i.e. the channel dimensions, flow rate and pressure) and chemical parameters (i.e. type and concentration of the surfactant).

In 2013 Colosi and coworkers (20) used a microfluidic foaming technique to generate highly monodispersed gas bubbles which were used as a template to manufacture poly(vinyl alcohol) (PVA) scaffolds with an ordered and homogeneous texture. Aqueous solutions of PVA containing a cationic surfactant (cetyl trimethyl ammonium bromide) and argon gas were simultaneously injected at constant flow rate into a flow-focusing device to produce monodispersed bubbles and foams which were frozen in liquid nitrogen, freeze dried and then cross-linked with glutaraldehyde to give a porous material. A comparison between this scaffold and one produced from PVA using a traditional foaming technique revealed that the
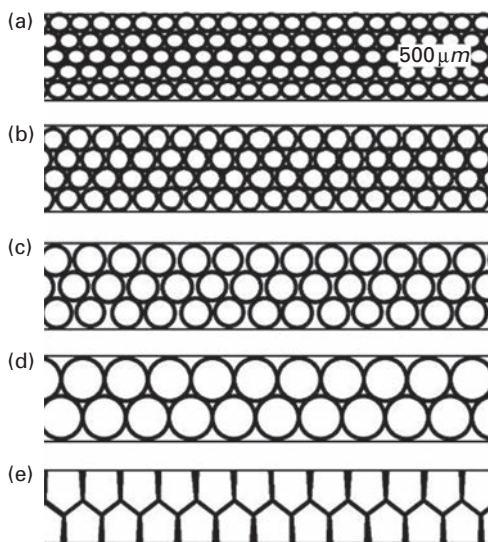
Fig. 5.24   Overlapped normalized histograms of the pore diameter of two PVA scaffolds, the darker represents the microfluidic foaming and no shade represents the gas foaming. From ref (20).

Fig. 5.25   The microfluidic flow-focusing device (top view). The cross-sections of the channels are rectangular. The widths of the inlet channels were set to $W_\ell = 250$ µm and $W_g = 200$ µm for the liquid and gas, respectively. Several widths of the orifice and outlet channel were used, and all devices had the same height, $h = 28$ µm. (b) Illustration of a bubble in the outlet channel. Bubbles are squeezed between the top and bottom walls and have a disc-like geometry. From ref (21).

microfluidic-manufactured scaffold had a more uniform porosity and a narrower pore size, as shown in Fig. 5.24.

   In 2004, Garstecki and coworkers (21) described a microfluidic bubble generator (Fig. 5.25) based on a flow-focusing device incorporated directly into a microfluidic chip which was capable of delivering bubbles from a single orifice at very high frequencies (up to several hundred thousand bubbles per sec) with a low polydispersity index. Using this generator, the size and volume fraction could be controlled independently and a variety of regular structures were generated. It was suggested that in the outlet channel, the bubbles interact by elastic shape-restoring forces when colliding with each other and indirectly by affecting the liquid flow field. Bubbles were forced to distort their circular shape and the

Examples of the flowing lattices formed by the bubbles in the outlet channel. The outlet channel width is $W_{out} = 750$ μm, the orifice width $W_{or} = 30$ μm, and the pressure is set to a constant value of $p = 27.6$ kPa. The liquid flow rates were as follows: (a) 0.2, (b) 0.14, (c) 0.0278, (d) 0.0056 and (e) 0.0028 μL/ s. From ref (21).

flowing lattice become a dynamic assembled foam as shown in Fig. 5.26. The dynamics of break-up in flow focusing cannot be explained by the competition between the shear stress and the interfacial tension, but an alternative idea was suggested based on a balance between the Laplace pressure pulling the tip upstream of the orifice where it has a lower curvature.

5.7　Nucleation of gas bubbles

From a fundamental viewpoint, nucleation of gas from the liquid may occur by either a homogeneous or a heterogeneous nucleation process. Homogeneous nucleation occurs in the absence of nucleation agents and requires high supersaturation pressures, whereas heterogeneous nucleation occurs in the presence of different types of nucleation agents, such as small particulate impurities or pre-formed bubbles and at much lower supersaturation conditions. According to the Young–Laplace equation, gas molecules in the vapor phase inside bubbles are in equilibrium with gas dissolved in the surrounding liquid, and the pressure difference across the gas/liquid spherical interface relative to a planar interface is related to the surface tension of the solution and the size of the bubble. Due to the curvature effect, the solubility of a gas in a liquid above a small bubble is much higher than the solubility in a liquid above a large bubble. For example, for a gas bubble of radius $r = 1$ mm (10^6 nm), ΔP has a value of 14.6 kPa, whereas for a smaller bubble with $r = 10$ nm, it is $\Delta P = 1.46 \times 10^4$ kPa, and as the bubble size is further reduced the pressure difference

increases toward an infinite value. Therefore, in order for homogenous nucleation to occur, according to the above reasoning, extremely high pressures are required to push out the gas from the solution, and for the smallest nuclei to form spontaneously (in the range of 2 nm) a pressure of about 1.46×10^5 kPa (or 10^3 bar) would be required. Clearly, this is impossible to achieve in bulk solution.

However, heterogeneous nucleation readily occurs at lower oversaturation levels and this take place in beverages such as beer and sparkling wines. In these drinks, it is the yeast and sugar which cause fermentation, and carbon dioxide is solubilized in the wine under an external pressure which builds up to a maximum value of 8 bar. Alcohol is also produced, and this reduces the surface tension to about 45–50 mN m^{-1} at room temperature. In such beverages, heterogeneous nucleation can occur by different methods, for example, by the entrapment of bubbles during the transfer of the pressurized liquid to another container. Another possibility discussed by Lyklema (22) concerns the presence of remnants of air bubbles that have been shrunk by Oswald ripening until the surface is fully covered by solid particles (impurities) that have become attached and stabilize the bubbles. Particulate impurities can also be suspended in solution or freely floating on the liquid surface. Heterogeneous nucleation can also occur from gas pockets which remain in crevices in the walls of glass or ceramic containers. However, this can occurs only under special circumstances, since the entrapment and release of the gas bubble is critically dependent on the size and geometry of the cavity in the container and the surface tension of the liquid. In fact, a key parameter is the radius of the pre-existing gas cavity on the walls of the vessel or on the suspended particulate, and this must exceed a critical value so that it overcomes the energy barrier and the build-up of pressure, thus enabling the bubble to grow.
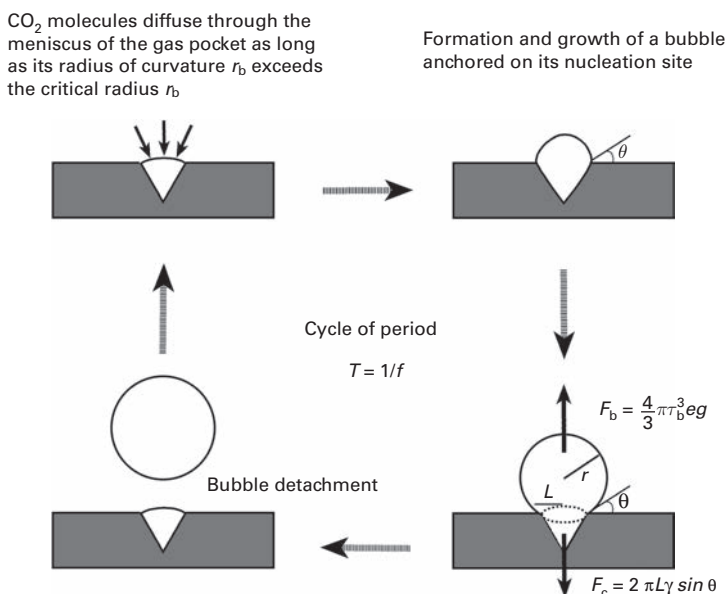
The wetting and curvature of the liquid in the cavity can be defined by Young's equation (23), shown below, which can be used to describe the wetting of a solid surface by a bubble and relates the contact angle θ between gas, water and solid surface to the three interfacial tensions $\gamma_{\text{gas/solid}}$, $\gamma_{\text{liquid/solid}}$ and $\gamma_{\text{gas/ liquid}}$.

$$\gamma_{\text{liquid/solid}} = \gamma_{\text{gas/sol}} + \gamma_{\text{gas/liquid}}\cos \theta \tag{5.6}$$

Provided the contact angle with air is fairly small, very small quantities of air can become trapped in pits or crevices of the solid. In this case, the Laplace pressure will be negative (negative curvature) and, upon coming into contact with the saturated liquid, the gas starts to diffuse from the bulk solution into the pocket and bubbles start to form and grow. After the bubble reaches a critical size, it is dislodged due to buoyancy, but small pockets remain so that one small air pocket can produce numerous bubbles. The mechanism of homogeneous cyclic nucleation is shown in Fig. 5.27.

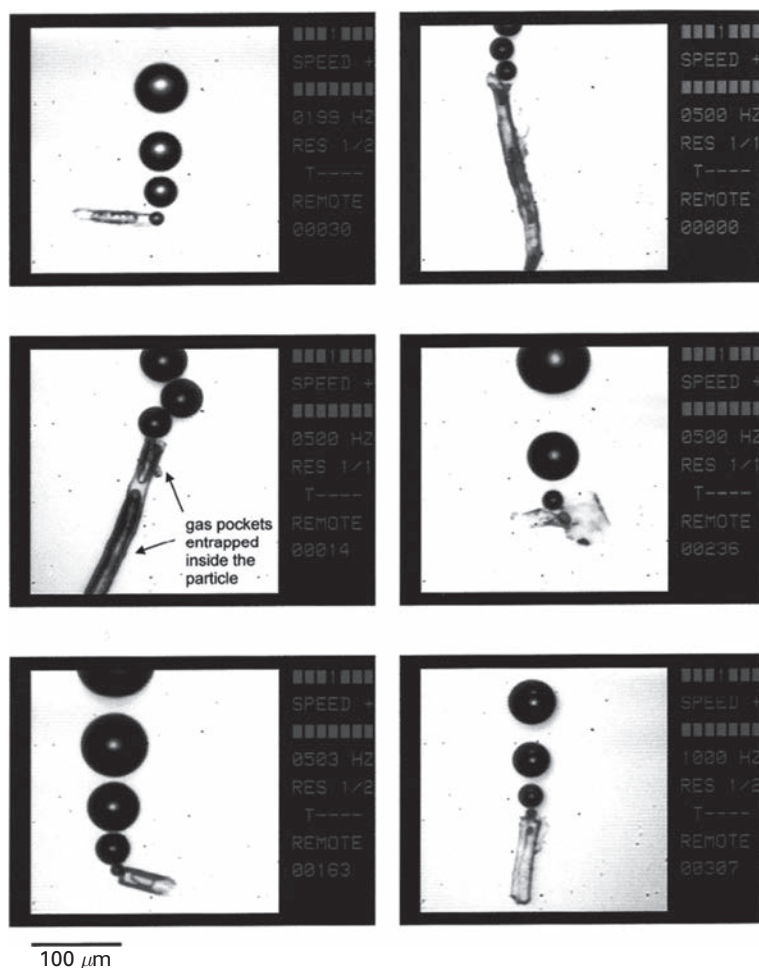### 5.7.1 Nucleation of bubbles in champagne and other beverages

In recent years there has been an intense effort to understand the underlying principles in the production and release of bubbles in champagne and to define the main physical

Fig. 5.27 The mechanism of cyclic nucleation of gas bubbles from a gas pocket. F_b is the buoyancy and F_c is the capillary force attaching the bubble to the cavity. From ref (24).

chemical parameters which control the size and flow of bubbles in a glass flute. Essentially, these studies have been focused on three important steps: (a) the nucleation process, (b) the bubble assent and (c) the bubble collapse at the free surface of the beverage. A great deal of work has been carried out in France by Liger-Belair and coworkers (24, 25, 26) at the University of Reims. Both champagne and sparkling wine contain supersaturated carbon dioxide, but the taste is quite different from still non-effervescent wine, and this is mainly due to the larger number of bubbles released which continuously rise in the beverages. Although it is generally accepted that the ascending bubbles in champagne are visually appealing, it is thought that the effervescence goes beyond esthetics, and these drinks actually taste different from still non-effervescent wine. In fact, it has been suggested that the huge numbers of bubbles which are released and continuously ascend through the liquid plays an important role in the flavor-releasing process. When bubbles reach the surface and burst via complex hydrodynamic processes, tiny droplets are released into the air, and the aroma (which comes from the organic surfactant components) is transferred into the vapor phase that is collected in the nose and mouth.

It was clearly shown in these studies that the heteronucleation of bubbles occurs in champagne at pre-existing cavities on the surface of the glass and from vapour and gas trapped inside hollow and minute submerged cellulose fibers. The tiny fibres appear as roughly cylindrical hollow threads about 100 microns in length with a cavity mouth of a few microns. These fibers or lumen are usually deposited as residuals after wiping the glass with a towel and probably adhere to the flute wall by electrostatic forces. In addition to fibers, natural effervescence may arise from gas pockets trapped inside
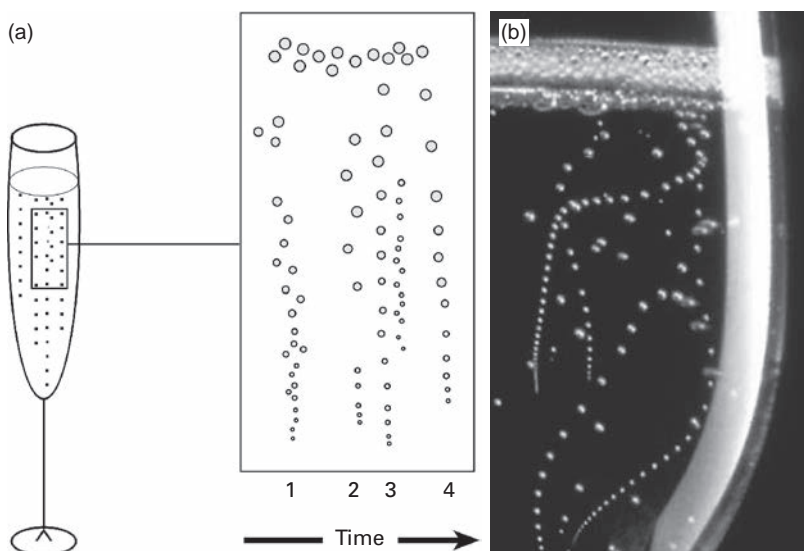
Fig. 5.28 Six particles acting as nucleation sites in a glass poured with champagne. Gas pockets entrapped inside the particles appear, and when a bubble is ejected a portion of the gas remains inside the particle. From ref (24, 25).

tartrate crystals precipitated on the glass wall during evaporation after rinsing the glass with tap water. From detailed observations, it was found that when the gas pocket reaches the tip of the fiber, a bubble is ejected but a portion of the gas remains inside the lumen, as shown in Fig. 5.28. Later, the gas pocket shrinks back to its initial position.

Careful optical analysis of the site characteristics enabled these workers to indirectly deduce the radii of curvature of the menisci in the cavity which act as nucleation sites. In addition, further analysis of the frequencies of the bubble formation and bubble growth rates in bubble trains enabled the length scale of the microscopic sites to be quantified. It was also reported that the rising bubbles grow by continuously absorbing carbon dioxide molecules from the liquid matrix and also that some fluid drains during their ascent to the free surface. Based on these

Fig. 5.29   (a) For many champagne connoisseurs, smaller bubbles streaming like chains of pearls is a measure of quality. This diagram shows the evolution of the bubble stream over time. (b) Close-up of bubble trains in motion in the champagne bulk.

observations it was possible to model the repetitive bubble nucleation process from a cellulose fiberm and the theoretical dependence of the bubbling frequency could be related to temperature and pressure. A constant release of bubbles from cellulose fiber can result in very complex rhythmical bubbling regimes. After pouring champagne into the flute the bubble trains rising toward the liquid surface show abrupt transitions from a few seconds to several minutes. This causes the bubble production to occur in cycles following a certain induction time period, as shown in Fig. 5.29, until it eventually stops due to lack of dissolved gas.

In addition to natural heterogeneous nucleation, artificial bubble nucleation can occur due to imperfections that were created intentionally by the glassmaker to replace a naturally occurring nucleation site (defect). Brewers have also experimented with the deliberate introduction of such pit-like defects in the glass surface in order to achieve better control of the process which otherwise depends on the age and conditions of the glass. Sandblasting or laser engraving the surfaces causes more vigorous and chaotic bubble nucleation than bubbling produced by tiny cellulose fibres.

5.7.2   Dissolved air and column flotation

Dissolved air flotation (DAF) involves the pre-saturation of water with air at high pressures. This is then fed through a needle valve or special orifices, causing a reduction in pressure and the nucleation of clouds of fairly small bubbles (about 50 to 80 microns in diameter). The process has a wide range of applications; for example, in the clarification of wastewater, the separation of solids in drinking water, the separation

of biological flocs, the removal and treatment of ions, the treatment of ultrafine minerals, the removal of oils and organics and the removal of algae and humic acids. It has been established that the size of the bubble generated in DAF is dependent on several parameters such as the air saturation pressure, the pressure reduction at the constriction, the nozzle design and the inlet water injection pressure (27). DAF has also been used to float hydrophilic particles such as quartz, which are easily coagulated by the hydrolyzing metal ions (iron and aluminum). Kitchener and Gochin (28) showed that the floatability of metal hydroxide precipitates was also sensitive to organic impurities which formed insoluble hydrophobic soaps that provide sites for bubble adhesion.

In recent years, DAF flotation in columns has been proved to be an important advancement in flotation (29), and the first effective columns were commercialized in 1979 to recover phosphate minerals. In column flotation, the bubbles are generated in the base of the column; at the upper part there is a pulp distributor to disperse the mineral particles and an elution device. Different types of bubble generators such as external bubble generators and in-line static mixtures have been introduced to the designs. The pulp (conditioned with reagent) is fed at a level of about two-thirds of the column height and becomes evenly distributed in the column. As the particles sink, they collide with the rising swarm of bubbles. The hydrophobic particles adhere and are transported to the froth layer, but the hydrophilic non-floatable particles continue to sink and are removed from the base of the column. Entrained less hydrophobic particles are washed back into the pulp by a downward flow of water in the column. Also, washing water from the elution device helps in reducing the contamination in the concentrate. The bubble size and concentration have an important influence on
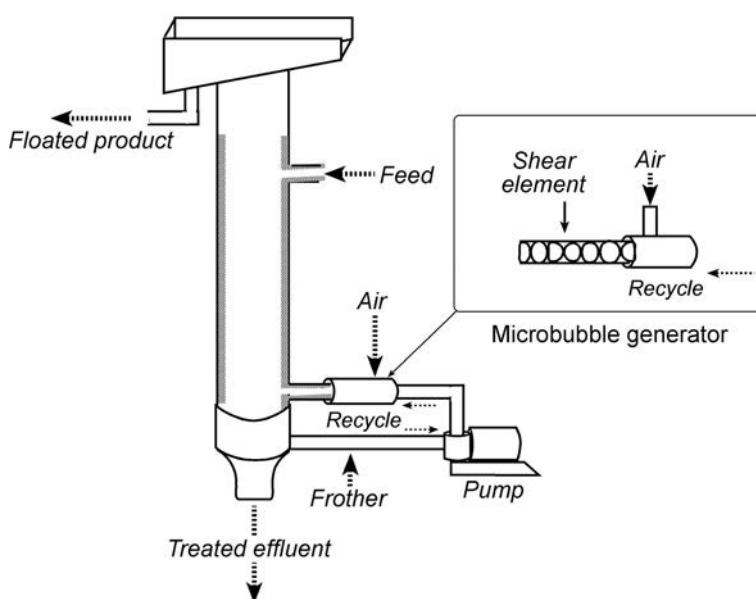

Fig. 5.30   The Microcel flotation column. From ref (29).

the flotation performance, and it is these parameters that increase the collision rate (collection rate) and the throughput of the process.

Yoon and coworkers (30) at Virginia State University successfully developed flotation columns fitted with microbubble generators to produce clean coal from high clay content refuse streams derived from the coal industry. In Fig. 5.30, a Microcel flotation column is depicted. It is through this column that microbubbles were generated by liquid cavitation in which a fast-moving stream of liquid is forced through a venturi to which air is injected at the point of lowest pressure. A microfoam (consisting of microbubbles with average diameter 25 microns) is produced after repeated cavitation and recirculation of a surfactant solution using this type of column.

New developments have been achieved in column technology by including external gas spargers which operate with and without surfactant or chemical frothing agents. Column flotation is used in many new application areas such as in the treatment of industrial effluents, oil removal in production of water and in the recovery of heavy metals.

5.8   In situ generation of foams by chemical reactions

Thermoplastic and polymer foams are commonly fabricated by chemical-blowing agents that decompose and release gas which dissolves in the melt under pressure. The melt is passed through a manufacturing dye during which the pressure is reduced, generating foam. Lower-density foams utilize chemical liquid- or gas-blowing agents (physical blowing gases) which are often injected into the molten plastic. The gas must be soluble at high pressures and temperatures, and must also become partially soluble as the pressure is reduced so that nucleation is initiated. During the foaming process, the type of gas, gas content, processing conditions and foaming dynamics all affect the final structure and morphology of the foam. Unfortunately, the process has been developed mostly by trial-and-error testing, and the physical/chemical principles are yet not fully understood. However, there are several publications which serve as a useful guides to comprehend the physics, chemistry and engineering involved in the process.

Although foamed materials can be manufactured fairly easily at low cost, the manufacturing steps are complex and very sensitive to external influences. Slight changes in environment, such as thermal, pressure, wetting and interfacial properties, can cause changes in the processing conditions. These may cause changes in the bubble expansion rate, diffusion, drainage and coalescence. If this occurs before loss of movement and solidification (quenching), then dramatic changes in the final foam structure may result. The type of polymer, the type of foaming or blowing agent, the expansion process and the post foam-curing can all influence the final product.

There has also been considerable effort aimed at understanding the relationship between final structure and interfacial processing in order to improve established manufacturing processes and generate new materials. The challenge is to identify the optimal processing conditions and steps which will generate the desirable
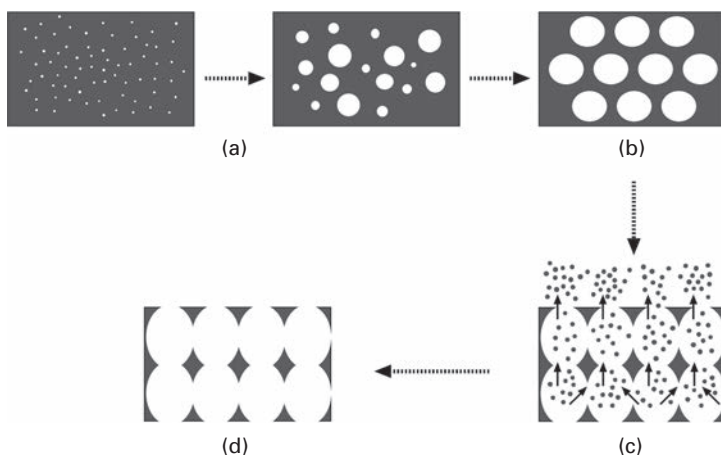
structures. The formation and preservation of the cell structure is an important step in processing the polymer. If bubbles are sparsely distributed in the foam, they will occur as spherical cells since this is the shape with the lowest surface energy. If the foam is less dense, then the cell will move toward a tetrahedral shape, with the wall stability being achieved by careful control of the factors that influence the membrane thinning. During processing, capillary action and drainage cause thinning, while an increase in the viscosity of the fluid reduces the drainage effects. Viscosity increases can result from chemical reactions that increase the molecular weight through polymerization or cross-linking or by temperature reduction. Ultimate bubble stabilization occurs as a result either of chemical reactions which continue to the point of gelation or from the physical effect of cooling.

Foaming agents are important additives in foamed thermoplastics. Such ("physical") foaming agents are low-boiling point liquids (pentane or isopropyl alcohol) that remain liquid when the melt is under pressure, but where the foaming agents change from liquid to vapor when the pressure is reduced. Other types of foaming agents include inert gases such as CO_2 or N_2. Chemical foaming agents utilize a chemical that decomposes to produce a gas or gases which then act similarly to physical foaming agents. It is also preferable that blowing agents are environmentally friendly and non-flammable. Gases with low diffusivity values produce stable foam structures. Pentane and butane gases have been used at room temperature but are flammable and have a high diffusivity through molten polyolefins, but more recently new methods of using pentane and butane have been developed. The diffusivity of close cell foams to gas or liquid can be related to foam structure. A selection of commercially used chemical foaming agents is given in Table 5.1.

Table 5.1 Examples of commercially used chemical foaming agents

Common name	Chemical name	endo-/exo-	Decomposition temperature (°C)	Gas evolution (cm^3/g)	Main foaming gas evolved
Citric acid/ Sodium bicarbonate	–	*endo-*	160–210	120	CO_2
ADCA	Azodicarbonate	*exo-*	205–212	220	N_2
OBSH	*p. p'*-Oxybis(benzene) sulfonyl hydrazide	*exo-*	158–160	125	N_2
TSH	*p*-Toluene sulfonyl hydrazide	*exo-*	110–120	115	N_2
TSS	*p*-Toluene sulfonyl semicarbazide	*exo-*	228–235	140	N_2
DNPT	Dinitrosopenta methylenetetramine	*exo-*	190	190	N_2
5PT	5-Phenyltetrazole	*exo-*	240–250	220	N_2
SBH	Sodium borohydride	*endo-*	–[a]	2000	H_2

[a] SBH is chemically activated by exposure to water.

Fig. 5.31   Macroscopic views of the different stages during polyurethane foaming: (a) bubble generation and growth, (b) packed bubble network (bubble expansion), (c) urea microphase separation (polymer stiffening) and cell opening, and (d) final curing. From ref (31).

In typical systems, such as polyurethane, the foam is produced by the polymerization of polyols with isocyanates, but it is necessary to provide "cell-openers" to obtain an open foam structure that does not shrink on cooling. In the manufacture of cold-hardening urea–formaldehyde foam plastics, an alkylnaphthalene acid derivative is used as a foam generation agent, although polyurethane products are also widely produced. During the processing of this foam, water reacts with the chemical isocyanate groups and produces carbon dioxide gas, which thus causes bubble expansion and occupies over 95% of the volume of the product. In the final stages, cell rupture occurs producing an open cell structure which solidifies. The different stages of the foaming process are shown in Fig. 5.31.

In addition to polymers and plastic foam systems, bubbles and foams are also produced by a range of chemical reactions in a wide range of industries. For example, disinfectant solutions that generate foams are prepared. Foams are also produced by chemical reactions, and frequently this can be detrimental in some industries; for example, slag foams are generated in electric arc furnaces, basic oxygen steelmaking and ladle processing in the steel industry. Although some slag foam is desirable in such processes for heat transfer, excessive foaming slows down production rates. The effects of bubble size and chemical reaction on slag foaming have been documented (32).

5.9   Gas generation by electrolysis

Gas-evolving electrodes are used in water hydrolysis, corrosion, electroflotation and metrology. Methods of bubble generation by electrolysis are usually more expensive
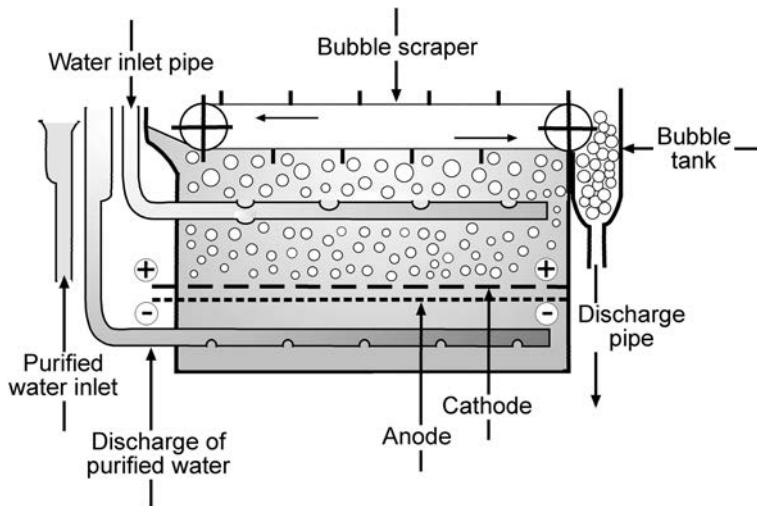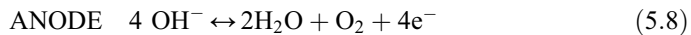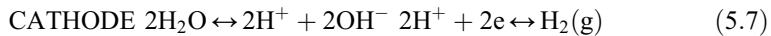
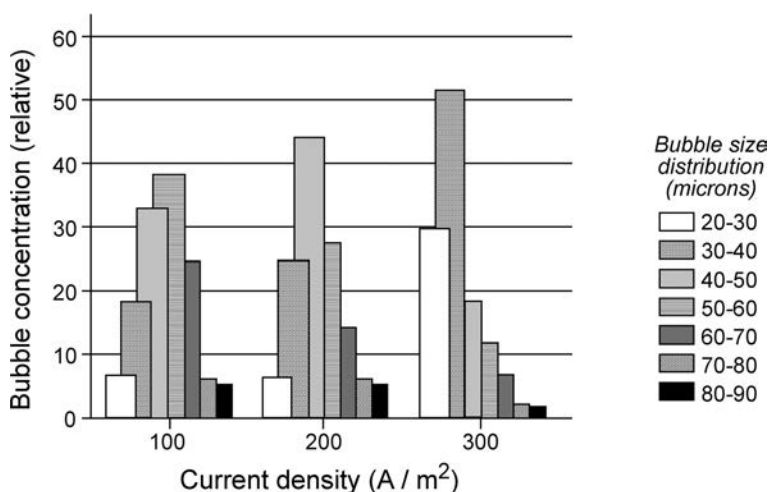**Fig. 5.32**   Single-cell electro-bubble generation cell. From ref (9).

than more conventional methods due to energy requirements. Most processes have been based on the electrolysis of water, with the cathode and anode reactions indicated as

$$\text{CATHODE } 2H_2O \leftrightarrow 2H^+ + 2OH^- \quad 2H^+ + 2e \leftrightarrow H_2(g) \tag{5.7}$$

$$\text{ANODE } \quad 4\,OH^- \leftrightarrow 2H_2O + O_2 + 4\,e^- \tag{5.8}$$

Hydrogen bubbles are created at minute defect sites on the electrodes, hydrogen at the cation and oxygen at the anode and, as the bubbles become detached, they rise to the surface of the cell increasing in size. The main parameters which control the size and number of electro-generated bubbles are current density, pH and electrode material. A typical electrochemical cell and bubble collector are shown in Fig. 5.32.

Interestingly, it has been demonstrated that very fine bubbles can be generated using electrolytic techniques compared to mechanical methods such as rotor stirrers, but the generation process is limited in that only oxygen and hydrogen can be produced. The empirical distribution of bubbles with respect to size was found to decrease with the density of the applied current, which also increased the number of bubbles generated (Fig. 5.33).

Industrial processes which utilize electrolysis for small-size bubble generation have been mostly employed for the separation of effluent and mineral particles. The technique has been applied to many different types of mineral systems such as sulfides, clays, fine diamond tailings and quartz with varying degrees of success. Several different types of flotation cells were developed in the former USSR for flotation of minerals. The cells need to operate at high current densities, preferably with low levels of gas released. However, a major disadvantage is that corrosion of the electrodes occurs after a period of time; this can be avoided to some extent by using electrodes consisting of, for example, Si-Fe, platinized titanium wire or Pt/Ir alloys.

Fig. 5.33   The size distribution of gas bubbles generated in an electrolysis cell at a range of current densities.

A range of alternative electrochemical cell architectures have been examined, for example, horizontal perforated sheets consisting of stainless steel and graphite, grid-expanded mesh and bipolar cells with vertical plates and membrane-separated electrode cells. These cells have been tested for the separation of a range of different types of minerals. In the United States, King (33) patented an electrolysis apparatus that produced good quality foam in tubes and channels using specially spaced electrodes of opposite polarity, enabling the bubbles to only escape from the surface of the cell. The apparatus was used for the treatment of pollutants, and the addition of surfactant to the cell was found to boost foam production.

Bubble growth during photoelectrochemical and electrolytic conversion processes has also been well studied (34, 35). It has been established that the size of a bubble grown from a surface in an electrolytic system can be expressed as $r_b = \beta t^a$, where r_b is the bubble size and t is the time and β and a are constants. However, it is usually difficult to control the process, and several studies have indicated that the surface area of the solid dominates the mechanism. The dynamics of the formation of a hydrogen single bubble at a platinum microelectrode was studied by Eckett and coworkers (36). Acid electrolytes were favored in contrast to alkaline which gave highly periodic rather than erratic bubble formation cycles. In 2014, Fernandez and workers (35) carried out a detailed study on the growth of hydrogen bubbles and their detachment from a platinum microelectrode using high-speed photography and over-potential frequency spectrum (noise) analysis. The periodic release of fairly large bubbles <800 μm, was recorded, and the release frequency was correlated with the bubble size and hydrogen production rate. In cases, the coalescence of bubbles at the electrode surface was inhibited chemically by surfactant or ethylene glycol or by hydrodynamically magneti-cally induced convection, and it was found possible to generate swarms of smaller bubbles of about 50 μm in aperiodic streams. The transition from periodic- to aperiodic-released bubbles appeared to be critically dependent on the surface tension, and it

occurred when the surface tension of the solution was lower than 70 mNm^{-1}. The controlled release of hydrogen gas bubbles from microelectrodes of pre-designed size and distribution could have potential applications in particle separation and ultrasonic imaging techniques.

References

(1) A. F. H. Ward, and L. Tordai, Time-Dependence of Boundary Tension of Solutions. 1. The Role of Diffusion in Time–Effects, *J. Chem. Phys.*, **14** (7), 453–461, 1946.

(2) R. Rao and P. Stenius, The Effect of Flotation Deinking Chemicals on Bubble Formation, *J. Pulp Pap. Sci.*, **24** (5), 156–160, 1998.

(3) D. Weaire and S. Hutzler, *The Physics of Foams*, Clarendon Press, Oxford, 1999.

(4) C. Wu, K. Nesset, J. Masliyah and Z. Xu, Generation and Characterization of Submicron Bubbles, *Adv. Colloid Interface Sci.*, **179**–182, 123–132, 2012.

(5) E. D. Hirst, R. K. Prudhomme and L. Rebenfield, Characterization of Foam Cell Size and Foam Quality using Factorial Design Analysis, *J. Dispersion Sci. Technol.*, **8**, 55–73, 1987.

(6) W. Hanselmann and E. Windhab, Flow Characteristics and Modeling of Foam Generation in a Continuous Rotor/Stator Mixer, *J. Food Eng.*, **38** (4), 393–405, 1999.

(7) N. Muller-Fischer and E. J. Windhab, Influence of Process Parameters on Microstructure of Food Foams Whipped in a Rotor-Stator Device within a Wide Static Pressure Range, *Colloids Surf.*, A, **263**, 353–362, 2005.

(8) C. Balerin, P. Aymard, F. Ducept, V. Vaslin and G. Cuvelier, Effect of Formulation and Processing Factors on the Properties of Liquid Food Foams, *J. Food Eng.*, **78**, 802–809, 2007.

(9) B. V. Deryagin and S. S. Dukhin, *Microflotation*, Khimiya, Moscow, 1986, as cited by S. Lu, R. J. Pugh and E. Forssberg, Interfacial Separation of Particles, Studies. In *Interface Science*, Vol. **20**, Elsevier Publications, 2005.

(10) H. Caps, N. Vanderwalle, G. Broze and G. Zocchi, Foamability and Structure Analysis of Foams in Hele-Shaw Cell, *Appl. Phys. Lett.*, **90** (21), Art No. 214101, May 21, 2007.

(11) H. Caps, Foaming Dynamics in Hele-Shaw Cells, N. Vandewalle and G. Broze, *Phys. Rev. E*, **73**, 065301 (R), 2006.

(12) N. Wallin, *Development, Adaption and Validation of a Test Method of Foam Formation, Food Technology*, Lund Institute of Technology, Lund University, Sweden and Tetra Pak Research and Development, Lund, Sweden, February 2005.

(13) O. Cheah and J. J. Cilliers, Foaming Behavior of Aerosol OT Solutions at Low Concentrations Using a Continuous Plunging Jet Method, *Colloids Surf., A*, **263**, 347–352, 2005.

(14) E. Dickenson, *Introduction to Food Science*, Oxford University Press, Oxford, UK, 1992.

(15) J. N. Lin, K. Banerji and H. Yasundra, Role of Interfacial Tension in the Formation and Detachment of Air Bubbles. 1. Single Orifice in a Horizontal Plane Immersed in Water, *Langmuir*, **10**, 936–942, 1994.

(16) J. N. Lin, K. Banerji and H. Yasundra, Role of Interfacial Tension in the Formation and Detachment of Air Bubbles. 2. A Single Orifice on an Inclined Plane Immersed in Water, *Langmuir*, **10**, 943–948, 1994.

(17) D. J. Tritton and C. Egdell, Chaotic Bubbling, *Phys. Fluids, A*, **5**, 503–505, 1993.

(18) I. Blute, R. J. Pugh, J. van de Pas J and I. Callaghan, Silica Nanoparticle Sols 1. Surface Chemical Characterization and Evaluation of the Foam Generation, *J. Colloid Interface Sci.*, **313**, 645–655, 2007.

(19) W. Drenckham and D. Langevin, Monodispersed Foams in One to Three Dimensions, *Curr. Opin. Colloid Interface Sci.*, **15**, 341–358, 2010.

(20) C. Colosi, M. Costantini, A. Barbette, R. Pecca, R. Bedini and M. Dentini, Morphological Comparison of PVA Scaffolds Obtained by Gas Foaming and Microfluidics Foaming Techniques, *Langmuir*, **29**, 82–91, 2013.

(21) P. Garstecki, I. Gitlin, W. DiLuzio and G. M. Whitesides, Formation of Mono-dispersed Bubbles in a Microfluidic Flow-Focusing Device, *Appl. Phys. Lett.*, **85** (13), 2649–2651, 2004.

(22) J. Lyklema, *Fundamentals of Interface Science and Colloid Science*, Vol. **V**, Soft Colloids, Elsevier Academic Press, Amsterdam, Holland, 2005.

(23) T. Young, An Essay on the Cohesion of Fluids, *Trans R. Soc. London*, **95**, 65, 1805.

(24) G. Liger-Belair, M. Vignes-Alder, C. Voison B. Robillard and P. Jeandet, Recent Advances in the Science of Champagne Bubbles, *Langmuir*, **18**, 1294–1301, 2002.

(25) G. Liger-Belair, M. Vignes-Adler, C. Voisin, B. Robillard and P. Jeandet, Kinetics of Gas Discharging in a Glass of Champagne: The Role of Nucleation Sites, *Chem. Soc. Rev.*, **37**, 2490–2511, 2008.

(26) G. Liger-Belair and P. Jeandet, Effervescence in a Glass of Champagne: A Bubbles Story, *Europhysics News*, pp. 10–15, January/February 2002.

(27) J. A. Solari and R. J. Gochin, Fundamental Aspects of Microbubble Flotation Processes. In *Colloid Chemistry in Mineral Processing*, Ed., J. S. Laskowsjki and J. Ralston, Elsevier, Amsterdam, Holland, Chapter 13, pp. 395–416, 1992.

(28) J. A. Kitchener and R. J. Gochin, The Mechanism of Dissolved Air Flotation for Portable Water; Basic Analysis and a Proposal, *Water Res.*, **15** (5), 585–590, 1983.

(29) J. Rubio, M. L. Souza and R. W. Smith, Overview of Flotation as a Wastewater Treatment Technique, *Minerals Eng.*, **15**, 139–155, 2002.

(30) R. H. Yoon, G. T. Adel and G. B. Luttrell, Process and Apparatus for Separating Fine Particles by Microbubble Flotation Together with a Process and Apparatus for Generating Microbubbles, US Patent 4,981,582, 1991; US Patent 5, 397, 001, 1995.

(31) X. D. Zhang, C. W. Macosko, H. T. Davies, A. D. Nikolov D and D. T. Wasan, Role of Silicon Surfactants in Flexible Polyurethane Foam, *J. Colloid Interface Sci.*, **215**, 270–279, 1999.

(32) Y. Zhang and R. J. Fruehan, Effect of Bubble Size and Chemical Reactions on Slag Foaming, *Metallurgical and Material Transactions, B*, **26**, (4), 803–812, 1995.

(33) A. S. King US Patent; 4,120,765, 1978; US Patent, 4,204, 940, 1980.

(34) N. Brandon and G. Kelsall, Growth Kinetics of Bubbles Electrogenerated at Microelectrodes, *J. Appl. Electrochem.*, **15** (4), 457–484, 1985.

(35) D. Fernandez and coworkers, Bubble Formation at a Gas Evolving Microelectrode, *Langmuir*, **30**, 43, 13065–13074, 2014.

(36) K. Eckert and coworkers, *Dynamics of Hydrogen Single Bubbles at a Platinum Microelectrode, Lecture 9. 6th Int. Workshop on Bubbles and Drop Interfaces*, Potsdam, Golm, Germany, July, 2015.